



**HAL**  
open science

## A lentiviral vector encoding fusion of light invariant chain and mycobacterial antigens induces protective CD4+ T cell immunity

Jodie Lopez, François Anna, Pierre Authié, Alexandre Pawlik, Min-Wen Ku, Catherine Blanc, Philippe Souque, Fanny Moncoq, Amandine Noirat, David Hardy, et al.

### ► To cite this version:

Jodie Lopez, François Anna, Pierre Authié, Alexandre Pawlik, Min-Wen Ku, et al.. A lentiviral vector encoding fusion of light invariant chain and mycobacterial antigens induces protective CD4+ T cell immunity. *Cell Reports*, 2022, 40 (4), pp.111142. 10.1016/j.celrep.2022.111142 . pasteur-03909608

**HAL Id: pasteur-03909608**

**<https://pasteur.hal.science/pasteur-03909608>**

Submitted on 21 Dec 2022

**HAL** is a multi-disciplinary open access archive for the deposit and dissemination of scientific research documents, whether they are published or not. The documents may come from teaching and research institutions in France or abroad, or from public or private research centers.

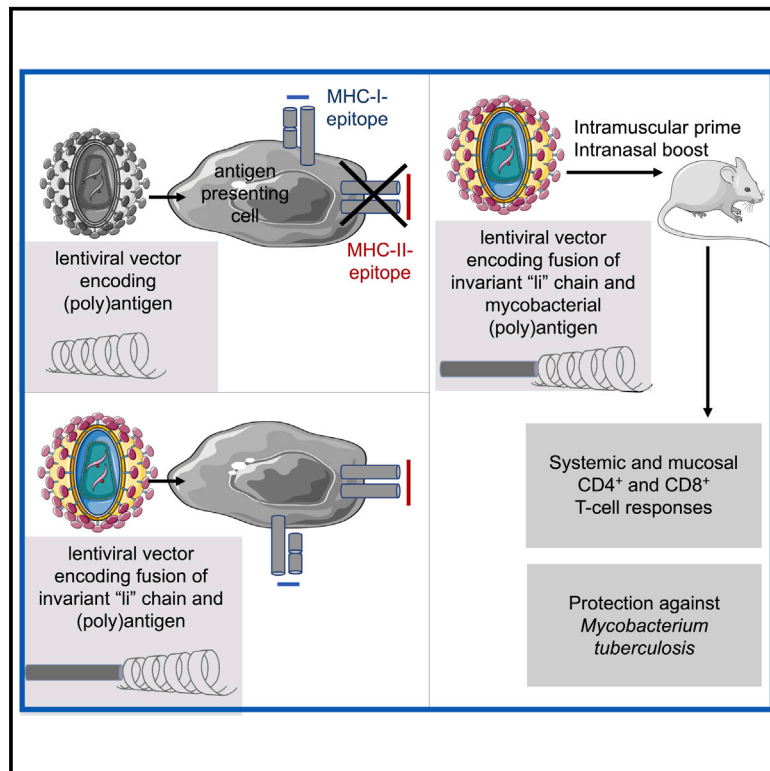
L'archive ouverte pluridisciplinaire **HAL**, est destinée au dépôt et à la diffusion de documents scientifiques de niveau recherche, publiés ou non, émanant des établissements d'enseignement et de recherche français ou étrangers, des laboratoires publics ou privés.



Distributed under a Creative Commons Attribution - NonCommercial - NoDerivatives 4.0 International License

## A lentiviral vector encoding fusion of light invariant chain and mycobacterial antigens induces protective CD4<sup>+</sup> T cell immunity

### Graphical abstract



### Authors

Jodie Lopez, François Anna, Pierre Authié, ..., Françoise Guinet, Pierre Charneau, Laleh Majlessi

### Correspondence

laleh.majlessi@pasteur.fr

### In brief

Lopez et al. show that lentiviral vaccination vectors encoding mycobacterial antigens attached to a component of a cellular antigen-presentation machinery display improved immunogenicity. Using antigens from *Mycobacterium tuberculosis* bacilli in this strategy, combined with intranasal vaccination, they observe protection potential against tuberculosis in mice.

### Highlights

- Conventional lentiviral vectors induce mainly MHC-I-restricted antigen presentation
- Fusion of the invariant li chain to antigen optimizes lentiviral vector immunogenicity
- Such optimized lentiviral vectors are suitable for mucosal CD4<sup>+</sup> T cell induction
- These lentiviral vectors induce anti-tuberculosis protection in mice



## Article

# A lentiviral vector encoding fusion of light invariant chain and mycobacterial antigens induces protective CD4<sup>+</sup> T cell immunity

Jodie Lopez,<sup>1</sup> François Anna,<sup>1</sup> Pierre Authié,<sup>1</sup> Alexandre Pawlik,<sup>2</sup> Min-Wen Ku,<sup>1</sup> Catherine Blanc,<sup>1</sup> Philippe Souque,<sup>1</sup> Fanny Moncoq,<sup>1</sup> Amandine Noirat,<sup>1</sup> David Hardy,<sup>3</sup> Wladimir Sougakoff,<sup>4</sup> Roland Brosch,<sup>2</sup> Françoise Guinet,<sup>5</sup> Pierre Charneau,<sup>1,6</sup> and Laleh Majlessi<sup>1,6,7,\*</sup>

<sup>1</sup>Institut Pasteur-TheraVectys Joint Lab, Université Paris Cité, 28 rue du Dr. Roux, 75015 Paris, France

<sup>2</sup>Institut Pasteur, Integrated Mycobacterial Pathogenomics Unit, CNRS UMR 3525, Université Paris Cité, 25 rue du Dr. Roux, 75015 Paris, France

<sup>3</sup>Institut Pasteur, Histopathology Platform, Université Paris Cité, 28 rue du Dr. Roux, 75015 Paris, France

<sup>4</sup>Sorbonne Universités, UPMC Université Paris 06, CIMI-Paris, AP-HP, Hôpital Pitié-Salpêtrière, CNR-MyRMA, 75013 Paris, France

<sup>5</sup>Institut Pasteur, Lymphocytes and Immunity Unit, Université Paris Cité, 25 rue du Dr. Roux, 75015 Paris, France

<sup>6</sup>Senior author

<sup>7</sup>Lead contact

\*Correspondence: [laleh.majlessi@pasteur.fr](mailto:laleh.majlessi@pasteur.fr)  
<https://doi.org/10.1016/j.celrep.2022.111142>

## SUMMARY

Lentiviral vectors (LVs) are highly efficient at inducing CD8<sup>+</sup> T cell responses. However, LV-encoded antigens are processed inside the cytosol of antigen-presenting cells, which does not directly communicate with the endosomal major histocompatibility complex class II (MHC-II) presentation pathway. LVs are thus poor at inducing CD4<sup>+</sup> T cell response. To overcome this limitation, we devised a strategy whereby LV-encoded antigens are extended at their N-terminal end with the MHC-II-associated light invariant chain (Ii), which contains an endosome-targeting signal sequence. When evaluated with an LV-encoded polyantigen composed of CD4<sup>+</sup> T cell targets from *Mycobacterium tuberculosis*, intranasal vaccination in mice triggers pulmonary polyfunctional CD4<sup>+</sup> and CD8<sup>+</sup> T cell responses. Adjuvantation of these LVs extends the mucosal immunity to Th17 and Tc17 responses. A systemic prime and an intranasal boost with one of these LV induces protection against *M. tuberculosis*. This strategy improves the protective power of LVs against infections and cancers, where CD4<sup>+</sup> T cell immunity plays an important role.

## INTRODUCTION

Replication-defective and non-cytopathic lentiviral vectors (LVs) are enveloped single-stranded RNA (ssRNA) viral particles that provide the basis for powerful gene delivery systems and immunization tools (Hu et al., 2011; Ku et al., 2021e). The properties that make LVs attractive as a vaccine platform are: (1) their very low genotoxic potential, (2) their capacity to accommodate large inserts, (3) their outstanding potential for gene transfer to the host cell nucleus, (4) their strong ability to transduce *in vivo* both dividing and non-dividing cells, including dendritic cells (DCs) (Esslinger et al., 2002; He et al., 2005), and (5) the absence of preexisting anti-vector immunity in human populations (Arhel et al., 2007; Di Nunzio et al., 2012; Hu et al., 2011; Ku et al., 2021e; Sirven et al., 2000; Zennou et al., 2000, 2001). In fact, LVs are mainly pseudotyped with the envelope glycoprotein of vesicular stomatitis virus (VSV), to which human populations are barely exposed (Hastie et al., 2013). LVs display *in vivo* tropism for DCs and are able to induce long-lasting antibody and CD8<sup>+</sup> T cell immunity (Ku et al., 2020, 2021b, 2021c).

We previously demonstrated that a single systemic administration of an LV encoding the Zika virus premembrane (prM) and envelope glycoprotein (E) provided complete and long-term protection against a Zika virus challenge in the murine model (Ku et al., 2020). More recently, we described that an LV encoding the full-length sequence of the Spike glycoprotein of SARS-CoV-2 induced strong neutralizing antibodies and poly-specific CD8<sup>+</sup> T cell responses. When administered to golden hamsters as a systemic prime followed by an intranasal (i.n.) boost, this vaccine candidate achieved complete eradication of SARS-CoV-2 in the lungs and alleviated pulmonary inflammation and pneumopathy (Ku et al., 2021d). Even a single i.n. injection of the vaccine was able to provide full and sustained protection to hamsters (Ku et al., 2021a). In addition, this LV vaccine candidate, used as an i.n. booster, fully prevented viral replication in the brain of transgenic mice known to be highly susceptible to SARS-CoV-2 in the central nervous system (Ku et al., 2021b). In these viral infectious diseases, the main correlates of protection are neutralizing antibodies and CD8<sup>+</sup> T cell responses.



Following host cell viral infection or LV-mediated transduction, the viral or transgenic antigens are synthesized in the cytosol on ribosomes and degraded by proteasomes. The proteolytic segments derived from them are then translocated into the endoplasmic reticulum. After possible trimming by aminopeptidases, the peptides with appropriate anchor residues and suitable length will bind to major histocompatibility complex (MHC)-I molecules, which will be ultimately displayed on the cell surface for antigenic presentation to specific CD8<sup>+</sup> T cell clones (Dhatchinamoorthy et al., 2021). These events fail to target the viral or transgenic antigens to the MHC-II presentation machinery, mainly located in the endosomal pathway. Therefore, viral vectors, including LVs, are usually not good inducers of CD4<sup>+</sup> T cell responses. However, these cells play major parts in the development and regulation of innate and adaptive immune responses, including the immune control of intracellular bacterial pathogens (Shepherd and McLaren, 2020). Here, we describe LVs capable of productively targeting encoded immunogens toward the MHC-II machinery, due to the addition of the MHC-II light invariant chain (Ii) to the N-terminal part of the antigen(s). This strategy is based on the well-established properties of the cytoplasmic portion of Ii that induce its diversion from the Golgi apparatus to the endosomes (Cresswell and Roche, 2014). As model antigens, we selected several immunogens from the intracellular pathogen *Mycobacterium tuberculosis* (Mtb), the control of which essentially requires the action of CD4<sup>+</sup> T cell responses *in vivo*. These optimized LVs, used in immunization strategies via the systemic or nasal route, allowed proper implementation of antigen trafficking to the MHC-II machinery, thereby eliciting, in addition to CD8<sup>+</sup> T cells, appropriate CD4<sup>+</sup> T cells that we characterized for their phenotype, functions, and pulmonary localization. A subcutaneous (s.c.) prime, followed by an i.n. boost with one of these improved LVs, induced significant levels of protection against Mtb in the murine model. The ability of these optimized LVs to induce both CD4<sup>+</sup> and CD8<sup>+</sup> T cell immunity, combined with the very low proinflammatory properties of these vectors, make them the vectors of choice for triggering multifunctional mucosal immunity at sites of pathogen entry or cancer development.

## RESULTS

### LV optimization to target antigens to the MHC-II pathway

To generate an LV-based immunization vector against Mtb, we selected the following virulence-related factors of Mtb: (1) EsxA and (2) ESX-1 secretion-associated protein (Esp) C, both secreted via the ESX-1 type VII secretion system (T7SS); (3) EsxH, secreted via the ESX-3 T7SS; (4) PE19, secreted via the ESX-5 T7SS; and (5) Ag85A, secreted via the Tat system (Abdallah et al., 2009; Banu et al., 2002; Cole et al., 1998; Groschel et al., 2016; Iantomasi et al., 2012; Majlessi et al., 2015). We first generated a conventional LV encoding a fusion of the five antigens (LV::TB). C57BL/6 mice were immunized with LV::TB, and their EspC-specific T cells were studied against the EspC:45-54 segment, which contains both MHC-I- and MHC-II-restricted epitopes in H-2<sup>b</sup> mice. Despite their EspC-specific CD8<sup>+</sup> T cells, no EspC-specific CD4<sup>+</sup> T cells were detected in these mice (Figure 1A). Additional LV constructs encoding individual EsxA, EspC, EsxH, PE19, or Ag85A, or various fusions of them, also

failed to trigger CD4<sup>+</sup> T cell responses (not shown). These observations are consistent with the poor ability of most viral vectors to deliver antigens to the MHC-II presentation pathway, despite their exceptional potential to target endogenously produced antigens to the MHC-I machinery.

To overcome LV inability to induce CD4<sup>+</sup> T cell responses, we sought to optimize this vector as detailed below. We used EsxH as the reporter antigen and the available EsxH-specific, MHC-I- or MHC-II-restricted T cell hybridomas to monitor antigen production and presentation (Table S1) (Hervas-Stubbs et al., 2006; Majlessi et al., 2003). We generated a series of LVs encoding: (1) EsxH alone (LV::EsxH); (2) EsxH fused at its N-terminal part to the murine MHC-II “Ii” (LV::Ii-EsxH), to target the translated antigen to the MHC-II endosomal compartment (Diebold et al., 2001; Rowe et al., 2006); (3) EsxH fused at its N-terminal part to the 1–118 transmembrane domain of the human transferrin receptor (LV::TfR<sub>1-118</sub>-EsxH), to generate a membrane-bound protein that should traffic through endosomes (Diebold et al., 2001; Rowe et al., 2006); or (4) EsxH fused at its N- and C-terminal ends, respectively, with HLA-B-derived leader SP peptide and MHC-I trafficking signal (LV::SP-EsxH-MITD), since the MHC-I molecules also traffic via endosomes (Kreiter et al., 2008) (Figures 1B and S1).

DCs transduced with each of the LV variants were able to productively present the MHC-I-restricted EsxH:20-28 epitope to a specific T cell hybridoma (Figure 1C). In contrast, only the optimized LV::Ii-EsxH and, to a lesser extent, LV::TfR<sub>1-118</sub>-EsxH were able to induce notable presentation of the MHC-II-restricted EsxH:74-88 epitope to a specific T cell hybridoma (Figure 1C). LV::SP-EsxH-MITD induced only a very weak antigen presentation, and the non-optimized LV::EsxH failed to present antigen in the context of MHC-II. For further experiments described below, we thus selected the Ii flanking strategy, which resulted in the highest MHC-II-restricted presentation level, without compromising the MHC-I-restricted presentation. Therefore, we identified a strategy to elaborate an LV with the added instrumental property of providing appropriate antigen presentation, i.e., “signal 1” (Liechtenstein et al., 2012), not only via MHC-I, but also via the MHC-II pathway.

### Weak proinflammatory but strong CD8<sup>+</sup> T-cell-immunogenic potential of LVs

Before exploring the potential of the optimized LV at inducing CD4<sup>+</sup> T cells *in vivo*, we assessed the ability of LVs to induce phenotypic or functional DC maturation, i.e., “signal 2–3” (Liechtenstein et al., 2012). Previously, a preparation of LVs not characterized for endotoxin content was described to induce moderate inflammatory responses *in vivo* (Cousin et al., 2019). Another study reported some degree of LV-induced DC maturation *in vitro*, attributed to the VSV G envelope glycoprotein, with which the LVs are pseudotyped (Pichlmair et al., 2007). Murine DCs, even when incubated with high amounts (MOI of 50) of our pre-GMP quality, VSV-G-pseudotyped LVs, displayed very modest phenotypic maturation, as judged by only a minor CD86 upregulation and minute increases in the percentages of MHC-I<sup>hi</sup> or MHC-II<sup>hi</sup> cells (Figures S2A–S2C). In terms of functional maturation, DCs transduced with LVs secreted IFN- $\alpha$ , CCL5, and IL-10 and very low amounts of IFN- $\beta$ . Importantly,

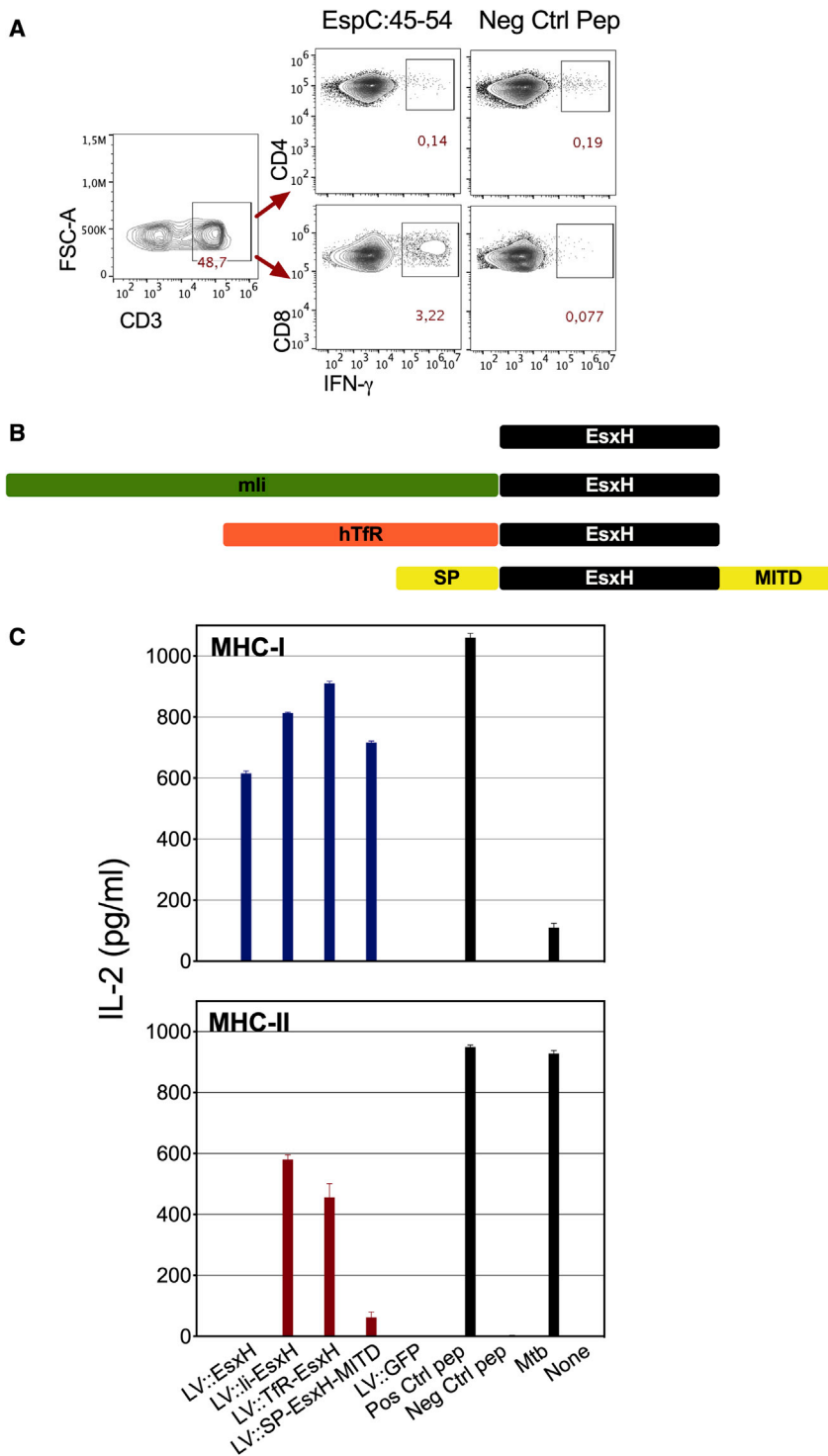


**Figure 1. Tailoring LVs to direct antigens toward the MHC-II processing pathway**

(A) Failure of conventional LVs to elicit CD4<sup>+</sup> T cells. Cytometric analysis of splenocytes from C57BL/6 mice immunized with a conventional LV coding for the fusion of EsxA-Ag85A-EspC-EsxH-PE19 Mtb immunogens. Shown are CD4<sup>+</sup> and CD8<sup>+</sup> T splenocyte IFN- $\gamma$  responses subsequent to *in vitro* stimulation with the EspC:45-54 peptide, which contains both MHC-I- and MHC-II-restricted epitopes in H-2<sup>b</sup>, or a negative control peptide.

(B) Scheme of full-length EsxH protein, with sequences potentially facilitating its routing through the MHC-II pathway added at its N- or C-terminal extremity.

(C) Presentation of MHC-I- or MHC-II-restricted EsxH epitopes by DCs (H-2<sup>d</sup>) transduced with  $1 \times 10^6$  TU/mL of LVs encoding EsxH alone, li-EsxH, TfR-EsxH, or SP-EsxH-MITD and co-cultured at day 3 post-transduction with T cell hybridomas specific to EsxH:20-28 and restricted by K<sup>d</sup> (YB8) (top) or specific to EsxH:74-88 and restricted by I-A<sup>d</sup> (1H2) (bottom). Results are the mean  $\pm$  SD of concentrations of IL-2, produced by T cell hybridomas after overnight co-cultures performed in technical quadruplicates. The experiment was repeated under the same conditions at least three times, with similar results.

See also [Figure S1](#) and [Table S1](#).

uniquely able to activate naive T cells, and how efficient LVs can be at promoting CD8<sup>+</sup> T cell responses (Ku et al., 2021e), we wondered whether CD8<sup>+</sup> T cell induction was dependent on DC IFN-I signaling. To this end, we used conditional C57BL/6 mutants, *ifnar1<sup>fllox/fllox</sup>* pCD11c-Cre<sup>+</sup> (with IFNAR-deficient DCs) versus *ifnar1<sup>fllox/fllox</sup>* pCD11c-Cre<sup>-</sup> (with IFNAR-proficient DCs), after confirmation that DCs derived from the former displayed largely reduced cell-surface IFNAR expression (Figure S3A). Mice, *ifnar1<sup>fllox/fllox</sup>* pCD11c-Cre<sup>-</sup> or Cre<sup>+</sup>, originating from the same litters, were immunized s.c. with  $5 \times 10^7$  transduction units (TU) of LV::OVA or LV::li-EsxH. Eleven days post-immunization (dpi), tetramer staining, ELISPOT, or intracellular cytokine staining (ICS) assays showed strong and comparable CD8<sup>+</sup> T splenocyte responses in both mouse types, specific to OVA (Figures S3B and S3C) or EsxH (Figures S3D–S3G). These include similar proportions of IFN- $\gamma$ <sup>+</sup> CD107a<sup>+</sup> degranulating or polyfunctional

CD8<sup>+</sup> T cells. The absence of correlation between the amounts of CD8<sup>+</sup> T cell response and IFNAR expression on DCs strongly suggests that the LV ability to induce CD8<sup>+</sup> T cell response does not result from IFNAR signaling in conventional DCs. Full IFNAR knockout (KO) mice have also been shown to mount

no IL-1 $\alpha$ , IL-1 $\beta$ , IL-6, or TNF was detected, indicating poor inflammatory and even anti-inflammatory properties of LVs (Figure S2D). Considering how LVs induce IFN-I production in DCs (Brown et al., 2007; Cousin et al., 2019) (Figure S2D), how DCs are

CD8<sup>+</sup> T cells. The absence of correlation between the amounts of CD8<sup>+</sup> T cell response and IFNAR expression on DCs strongly suggests that the LV ability to induce CD8<sup>+</sup> T cell response does not result from IFNAR signaling in conventional DCs. Full IFNAR knockout (KO) mice have also been shown to mount

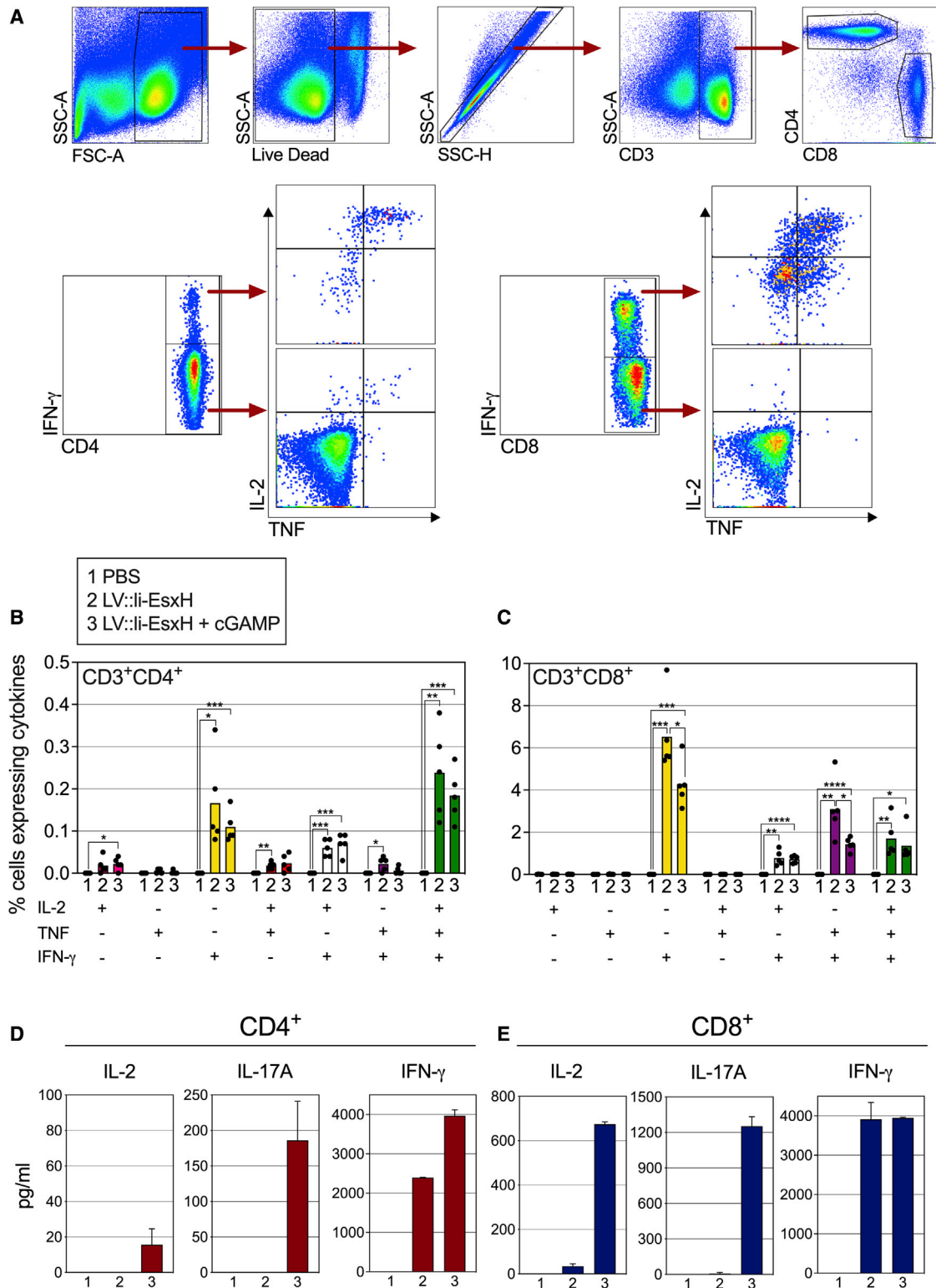


**Figure 2. Induction of systemic or mucosal CD4<sup>+</sup> and CD8<sup>+</sup> T cell responses by the optimized LV**

BALB/c (H-2<sup>d</sup>) mice (n = 5/group) were injected with PBS (1) or immunized s.c. with  $5 \times 10^8$  TU of LV::li-EsxH alone (2) or adjuvanted with cGAMP (3). At 11 dpi, EsxH-specific Th1 cytokine responses of splenocytes were analyzed by ICS in individual mice.

(A) Gating strategy carried out on cytokine-producing CD4<sup>+</sup> or CD8<sup>+</sup> T cells.

(legend continued on next page)

OVA-specific CD8<sup>+</sup> T cell responses as strong as those detected in their wild-type (WT) counterparts after immunization with LV::OVA (Cousin et al., 2019).

Therefore, even if LVs are very strongly immunogenic, their low DC-stimulatory capability highlights their intrinsically weak proinflammatory potential. In addition, LV-mediated T cell induction is not reliant on DC signaling through IFN-I, which is one of the few inflammatory mediators that they can produce.

### Strong capacity of the optimized LV to induce systemic and mucosal CD4<sup>+</sup> T cell immunity

We then evaluated the potential of the optimized LV::li-EsxH to induce CD4<sup>+</sup> T cell responses at the systemic or mucosal levels. Accounting for the mild impact of LV on the innate immune system, we evaluated LV::li-EsxH either alone or adjuvanted with the pro-Th1/Th17 cyclic guanine-adenine dinucleotide (cGAMP) (Van Dis et al., 2018). BALB/c mice were first immunized s.c. with  $5 \times 10^8$  TU of LV::li-EsxH, alone or adjuvanted. At 11 dpi, ICS analysis detected sizeable populations of EsxH-specific Th1 cytokine-producing CD4<sup>+</sup> (Figures 2A and 2B) and CD8<sup>+</sup> (Figures 2A and 2C) T splenocytes. Adjuvantation of LV::li-EsxH with cGAMP did not improve the frequencies of specific T cells after systemic immunization (Figures 2B and 2C). No T cell responses were detected in control mice injected s.c. with cGAMP alone (not shown).

Then, mucosal immunization of BALB/c mice was performed via the i.n. route with LV::li-EsxH, alone or adjuvanted. At 13 dpi, lung T cells were co-cultured with syngeneic DCs loaded with EsxH:74-88 or EsxH:20-28 peptides, bearing MHC-II or MHC-I H-2<sup>d</sup> T cell epitopes, respectively (Hervas-Stubbs et al., 2006; Majlessi et al., 2003). Mucosal antigen-specific IL-2- or IL-17A-producing CD4<sup>+</sup> T cells were detected only in the lungs of mice immunized with cGAMP-adjuvanted LV::li-EsxH (Figure 2D). In parallel, mucosal antigen-specific IL-2- or IL-17A-producing CD8<sup>+</sup> T cells were detected in the lungs of mice immunized with cGAMP-adjuvanted LV::li-EsxH (Figure 2E). Antigen-specific IFN- $\gamma$ -producing lung CD4<sup>+</sup> or CD8<sup>+</sup> T cells were detected in all immunized groups (Figures 2D and 2E). Therefore, although adjuvantation with cGAMP had no positive impact on the immunogenicity of LVs following systemic immunization, it helped to induce better mucosal responses following i.n. immunization.

Intravenous (i.v.) injection of mice with PE-anti-CD45 monoclonal antibody (mAb) 3 min before sacrifice allows the distinction of hematopoietic cells located inside the lung parenchyma from those in the lung vasculature (Anderson et al., 2014). Compared with the PBS-injected controls, mice immunized with LV::li-EsxH alone showed increased percentages of CD45<sub>i.v.</sub><sup>-</sup> CD4<sup>+</sup> (Figure 3A) or CD45<sub>i.v.</sub><sup>-</sup> CD8<sup>+</sup> (Figure 3C) T cells in the parenchyma. This T cell recruitment/expansion was further enhanced in mice immunized with adjuvanted LV::li-EsxH. Notable amounts of antigen-specific IFN- $\gamma$ /TNF-

producing CD4<sup>+</sup> (Figures 3B and 3E) or CD8<sup>+</sup> (Figures 3D and 3F) T cell effectors were detected in the parenchyma of mice immunized with LV::li-EsxH alone. Immunization with cGAMP-adjuvanted LV::li-EsxH generated higher proportions of Tc17 cells (Figures 3D and 3F). This observation is consistent with the release of IL-17A into the supernatants of lung T cells stimulated *in vitro* with EsxH:74-88 or EsxH:20-28 peptides (Figures 2D and 2E). CD45<sub>i.v.</sub><sup>+</sup> Th1 cytokine-producing CD4<sup>+</sup> or CD8<sup>+</sup> T cells were also detected in the vasculature (Figures 3B and 3D–3F), indicating that i.n. immunization can also generate antigen-specific T cells that gain access to the blood circulation and thus contribute to the systemic immunity.

### High potential of a polyantigenic-optimized LV to induce systemic and mucosal CD4<sup>+</sup> T cell immunity

We then generated an optimized LV encoding a fusion of li and juxtaposed sequences of EsxH, EsxA, EspC, and PE19 (LV::li-HAEP) (Table S2, Figure S1). LV::li-HAEP-transduced DCs were able to present the MHC-I- or MHC-II-restricted epitopes of these immunogens to specific T cell hybridomas (Figure S4A). As determined by ELISPOT, in C57BL/6 mice, systemic s.c. immunization with  $5 \times 10^8$  TU of LV::li-HAEP alone, i.e., without adjuvant, induced IFN- $\gamma$ /TNF-producing CD4<sup>+</sup> or CD8<sup>+</sup> T splenocytes specific to all included immunogens (Figure S4B), with notable bi- or polyfunctionality in both subsets (Figures S4C and S4D). Similar to LV-mediated CD8<sup>+</sup> T cell induction, we did not detect any dependence of CD4<sup>+</sup> T cell induction on DC IFNAR signaling with this optimized LV (Figure S5A). We also established that immunization via the s.c. or intramuscular (i.m.) systemic route with LV::li-HAEP alone resulted in comparable IFN- $\gamma$  or TNF CD4<sup>+</sup> and CD8<sup>+</sup> T splenocyte responses (Figure S5B).

Mucosal i.n. immunization of C57BL/6 mice with cGAMP-adjuvanted LV::li-HAEP ( $1 \times 10^9$  TU/mouse) elicited (poly)functional CD4<sup>+</sup> (Figure 4A) or CD8<sup>+</sup> (Figure 4B) T cells specific to each of the four Mtb antigens included in the LV construct. This response was found both in the lung parenchyma and in the lung vasculature. The CD45<sub>i.v.</sub><sup>-</sup> parenchymal CD4<sup>+</sup> or CD8<sup>+</sup> T subset in vaccinated mice contained increased proportions of CD27<sup>-</sup> CD62L<sup>-</sup> migrant effectors and CD69<sup>+</sup> CD103<sup>+</sup> lung-tissue-resident cells, compared with control animals (Figures 4C and 4D). The majority of CD69<sup>+</sup> CD103<sup>+</sup> CD4<sup>+</sup> T cells displayed a CD44<sup>+</sup> CXCR3<sup>+</sup> phenotype (Figure 4C, bottom), reminiscent of CD8<sup>+</sup> T cell resident-memory phenotype (Schenkel and Masopust, 2014; Turner et al., 2014). The majority of CD69<sup>+</sup> CD103<sup>+</sup> CD8<sup>+</sup> T cells also had a resident-memory phenotype (Figure 4D, bottom).

### Features of lung innate immune cells after i.n. LV administration

As determined by detailed cytometric analysis in individual mice at 1 dpi, 3 min after i.v. injection of mice with PE-anti-CD45 mAb

(B and C) Recapitulative frequencies of each (multi)functional population within the CD4<sup>+</sup> (B) or CD8<sup>+</sup> (C) T subset. Results represent means with individual values. \* $p \leq 0.05$ , \*\* $p \leq 0.01$ , \*\*\* $p \leq 0.001$ , \*\*\*\* $p \leq 0.0001$ ; statistical significance was determined by two-tailed unpaired t test.

(D and E) BALB/c mice ( $n = 3$ /group) were immunized i.n. with  $5 \times 10^7$  TU of LV::li-EsxH alone or adjuvanted with cGAMP. At 13 dpi, EsxH-specific lung CD4<sup>+</sup> or CD8<sup>+</sup> T cell responses were analyzed by co-culture of lymphocytes enriched from the lungs with homologous DCs loaded with EsxH:74-88 (MHC-II) (D) or with EsxH:20-28 (MHC-I) (E). IL-2, IL-17A, or IFN- $\gamma$  contents in the co-culture supernatants were quantitated by ELISA.

Results are the mean  $\pm$  SD. The experiment was repeated twice, with similar experimental groups and with comparable results. Injection of cGAMP alone did not induce a response.

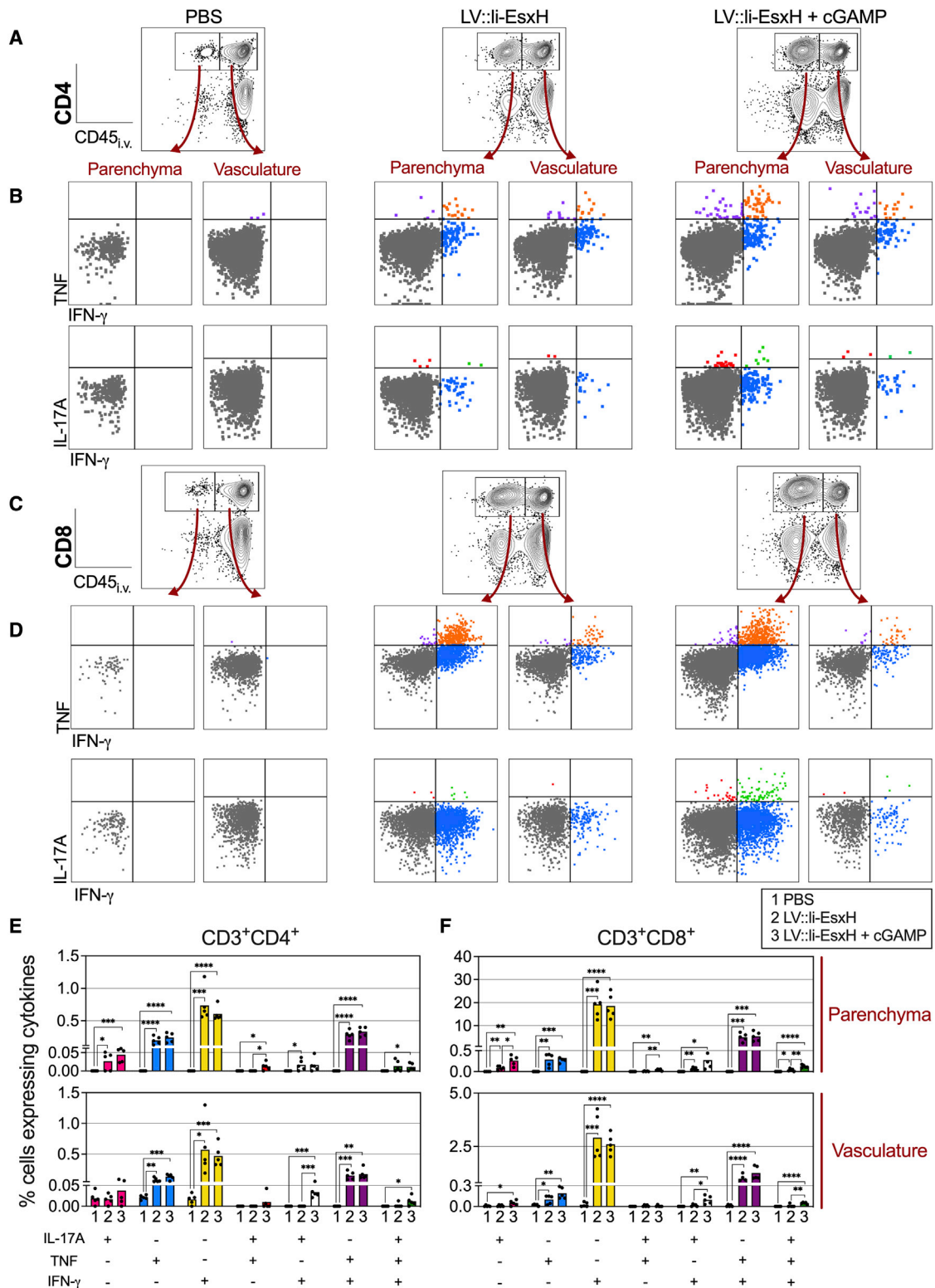


**Figure 3. Characterization of mucosal CD4<sup>+</sup> or CD8<sup>+</sup> T cell responses induced by the optimized LV**

(A–D) BALB/c (H-2<sup>d</sup>) mice (n = 5/group) were immunized i.n. with  $1 \times 10^9$  TU of LV::li-EsxH alone or adjuvanted with cGAMP. At 13 dpi, lung CD4<sup>+</sup> (A) or CD8<sup>+</sup> (C) T cells were discriminated for their location inside the parenchyma (CD45<sub>i.v.</sub><sup>-</sup>) or in the vasculature (CD45<sub>i.v.</sub><sup>+</sup>) by an i.v. injection of PE-anti-CD45 mAb, 3 min

(legend continued on next page)

3 min before sacrifice (Figure 5A), the only impact of i.n. administration of LV alone on lung innate immune cell subsets was a slightly significant increase in the total number of Ly6C<sup>+</sup> monocytes/macrophages and neutrophils and a statistically non-significant trend toward increased total numbers of interstitial macrophages and monocyte-derived DCs (Figure 5B). Addition of cGAMP to the LV resulted in a decrease in the number of lung DCs and a significant increase in the number of alveolar macrophages, interstitial macrophages, and their Ly6C<sup>+</sup> precursors, with potential roles in pathogen removal, antigen presentation, and possibly tissue repair, respectively.

To identify the cell subsets transduced *in vivo* by LVs following i.n. administration, C57BL/6 mice were immunized i.n. with  $5 \times 10^8$  TU of LV::GFP. Control mice received an empty LV (Ctrl LV). Lungs from individual mice were analyzed at day 4 post-immunization (Figures 6A and 6B). GFP<sup>+</sup> cells were mainly detected in alveolar and interstitial macrophages and plasmacytoid, CD11c<sup>hi</sup> CD103<sup>+</sup>, and CD11c<sup>int</sup> CD64<sup>-</sup> DCs (Figure 6C). These observations are in accordance with our previous results generated after i.m. or i.n. LV administration (Ku et al., 2021c; Vesin et al., 2022).

### Protective properties of a polyantigenic-optimized LV against Mtb

We had previously observed low levels of Ag85A expression in some Beijing Mtb clinical isolates, questioning the relevance of including this antigen in Mtb vaccine candidates (Sayes et al., 2018). Mtb Beijing family strains have been associated with strong virulence, transmission, and antibiotic resistance (Gagneux, 2018), and their characteristics have to be considered in vaccine design. To address this question, we quantitated the intraphagocyte secretion of Ag85A (Figure S6A) and also EsxA as another Mtb antigen (Figure S6B) inside DCs infected with each of the 15 non-Beijing strains, in comparison with the 31 Beijing clinical Mtb isolates listed in Table S3. Although the average level of Ag85A and EsxA expression of the Beijing clinical isolates was significantly lower than that of the non-Beijing strains, the level of expression of this antigen was wide-ranging, and many Beijing isolates were found to produce large amounts of Ag85A and also EsxA (Figure S6C). Therefore, we added the Ag85A:241-260 immunogenic region (D'Souza et al., 2003; Sayes et al., 2012) to the C-terminal end of HAEP in LV::li (LV::li-HAEP) (Figure S1F; Table S2). LV::li-HAEP-transduced DCs were able to induce MHC-II-restricted presentation of Ag85A:241-260, in addition to the presentation of the other Mtb antigens, as exemplified by EsxA and detected by reporter T cell hybridomas (Figure S6D).

We then evaluated *in vivo* the booster potential of cGAMP-adjuvanted LV::li-HAEP in C57BL/6 mice primed with BCG::ESX-1<sup>Mmar</sup>. This strain secretes, via the ESX-1 secretion system, the

EsxA and EspC antigens (Groschel et al., 2017) that are included in the HAEP multiantigen. A group of BCG::ESX-1<sup>Mmar</sup>-primed mice was boosted (s.c.) with  $5 \times 10^8$  TU of LV::li-HAEP at week 5 and then boosted again (i.n.) with LV::li-HAEP adjuvanted with cGAMP at week 10 (Figure S7A). At week 12, the mice were challenged via aerosol with  $\approx 200$  CFU of Mtb H37Rv. At 5 weeks post Mtb challenge, the lung mycobacterial loads in the primed and boosted mice showed a significant decrease compared with the mice vaccinated with only BCG::ESX-1<sup>Mmar</sup> (Figure S7B), albeit without major impact on lung histopathology (Figure S7C).

A second experiment was designed to evaluate the protective potential of LV::li-HAEP on its own if administered at a higher dose, and to increase the rest period between the last i.n. boost with adjuvanted LV::li-HAEP and the Mtb challenge, to distinguish a possible part of the protection resulting from the early innate immunity from a more persistent T cell immunity. C57BL/6 mice were: (1) left unvaccinated, (2) vaccinated s.c. at week 0 with  $1 \times 10^6$  CFU of BCG Pasteur, or (3) primed (s.c.) at week 0 with  $1 \times 10^9$  TU of LV::li-HAEP and boosted (i.n.) at week 4 with  $1 \times 10^9$  TU of LV::li-HAEP + cGAMP (Figure 7A). A control group received (s.c.) at week 0 and then (i.n.) at week 4 an empty Ctrl LV + cGAMP. Fifteen weeks after the i.n. boost, when the innate immunity linked to the adjuvanted vector could not interfere directly with the anti-mycobacterial defense, mice were challenged i.n. with  $1 \times 10^3$  CFU of Mtb H37Rv. At 6 weeks post-Mtb challenge, whereas a large reduction in mycobacterial loads was detected in the lungs and spleen of LV::li-HAEP primed-boosted mice, the organs of the mice injected with the Ctrl LV contained mycobacterial loads comparable to those in unvaccinated mice. These results highlighted the protective potential of the LV::li-HAEP-induced T cell immunity (Figure 7B).

This observation in the preclinical murine model encourages further evaluation of the protective potential of such optimized and multiantigenic LV in larger rodents or non-human primates. Altogether, the non-cytopathic and weakly proinflammatory properties of LVs and their optimization for CD4<sup>+</sup> T cell induction, as well as their optional adjuvantation, pave the way to multiple systemic and mucosal vaccine strategies.

### DISCUSSION

Despite their remarkable ability to target endogenously produced antigens into the MHC-I pathway of transduced antigen-presenting cells, viral vectors, including LVs, mostly fail to deliver antigens to the MHC-II machinery for CD4<sup>+</sup> T cell induction. Here, we describe LVs in which the genes encoding multiple immunogens were engineered to allow trafficking of the resulting fusion protein through the MHC-II pathway. Addition of the li or TfR at the N terminus of a single or a polyantigenic protein

before sacrifice. Cytokine production, as detected by ICS in lung CD4<sup>+</sup> (B) or CD8<sup>+</sup> (D) T cells of the lung parenchyma or vasculature, is shown. Injection of cGAMP alone did not induce a response.

(E and F) Recapitulative percentages of CD4<sup>+</sup> or CD8<sup>+</sup> T cells in the parenchyma or vasculature, as determined by ICS.

\* $p \leq 0.05$ , \*\* $p \leq 0.01$ , \*\*\* $p \leq 0.001$ , \*\*\*\* $p \leq 0.0001$ ; statistical significance was determined by two-tailed unpaired t test. We collected approximately  $5\text{--}16 \times 10^6$  cells in the lymphocyte-enriched fraction from lungs, and at least  $1 \times 10^6$  events per sample were acquired by cytometer. The experiment was performed three times: twice with pooled cells inside each experimental group and once shown here, which was performed on cells recovered from individual mice per group. See also Figures S4 and S5.

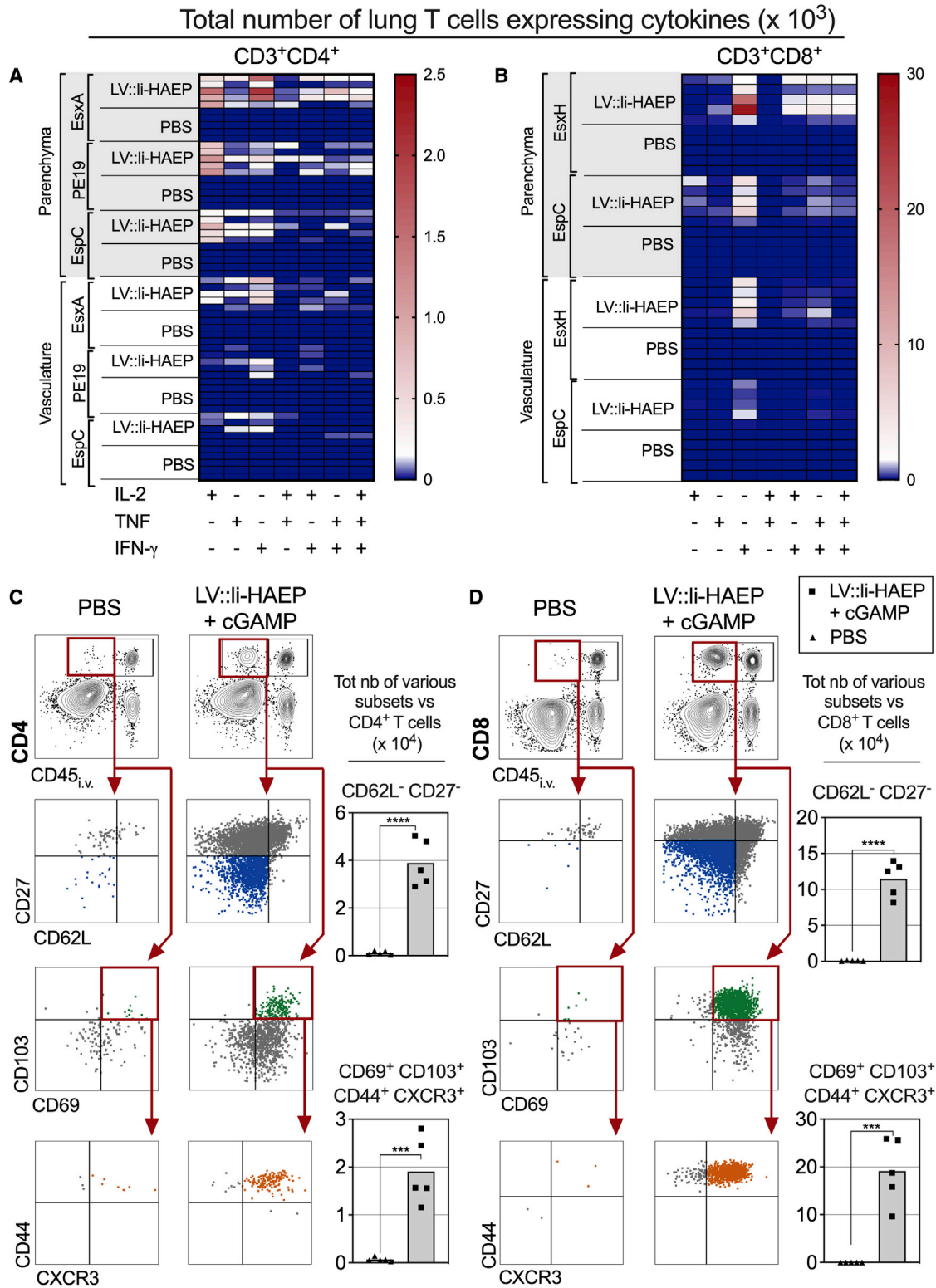


**Figure 4. Mucosal T cell responses induced by LV::li-HAEP**

C57BL/6 (H-2<sup>b</sup>) mice were immunized i.n. with  $1 \times 10^9$  TU of LV::li-HAEP, adjuvanted with cGAMP, or instilled with PBS (n = 5).

(A and B) At 13 dpi, following an i.v. injection of PE-anti-CD45 mAb 3 min before sacrifice, CD4<sup>+</sup> (A) or CD8<sup>+</sup> (B) lung T cell responses were analyzed by ICS after co-culture with homologous DCs loaded with EsxA:1-20 (MHC-II), PE19:1-18 (MHC-II), EspC:40-54 (MHC-I and -II), EsxH:20-28 (MHC-I), or an irrelevant negative

(legend continued on next page)

encoded by LVs achieved proper antigen routing to the MHC-II machinery and robust triggering of CD4<sup>+</sup> T cells, without reducing MHC-I presentation and CD8<sup>+</sup> T cell induction. In the context of an adenoviral vector, fusion of a hepatitis C virus antigen to li enhances both CD8<sup>+</sup> and CD4<sup>+</sup> T cell responses in non-human primates and humans, without development of anti-li antibodies or T cell responses (Capone et al., 2014; Esposito et al., 2020). The increase in CD8<sup>+</sup> T cell responses has been linked to enhanced ubiquitination and proteasomal degradation (Esposito et al., 2020). Another strategy has been the replacement of the CLIP (class II-associated invariant chain peptide) region of li by antigenic peptides, which improves peptide presentation via both MHC-I and MHC-II molecules (Mensali et al., 2019).

As model antigens, we selected Mtb-derived antigens because the major correlates of TB protection are CD4<sup>+</sup> T cells (Andersen and Scriba, 2019; Lewinsohn et al., 2017). The choice of the Mtb immunogens was based on their direct relationship with mycobacterial virulence *in vivo* and their active secretion by the ESX-1, ESX-3, and ESX-5 T7SS or Tat systems, through various phases of the disease (Lindestam Arlehamn et al., 2013; Majlessi et al., 2015). As a note of caution, we noticed that preservation of the native tertiary structure can be an important factor for the technique to work. For instance, LVs encoding a fusion of li and a cluster of predicted T cell epitopes from EsxH, EsxA, EspC, and PE19 Mtb antigens, and therefore enriched in hydrophobic sequences, failed to preserve protein folding and did not induce antigen routing to the MHC-II machinery (data not shown).

As we recently demonstrated with LV-based vaccination against SARS-CoV-2, systemic immune responses, even of high quality, may not always reach the site of infection in the lung mucosa to prevent replication of pulmonary pathogens (Ku et al., 2021b, 2021d; Majlessi and Charneau, 2021). Mucosal immunity, including antibodies and tissue-resident lymphocytes, has been shown to be instrumental in pathogen clearance from the respiratory tract (Chiu and Openshaw, 2015; Holmgren and Czerkinsky, 2005; Ku et al., 2021d; Mueller and Mackay, 2016; Park and Kupper, 2015). Moreover, the protection against pulmonary TB has been correlated with the presence in the lung of antigen-specific resident-memory CD4<sup>+</sup> T cells (Bull et al., 2019; Florido et al., 2018; Perdomo et al., 2016; Sakai et al., 2014). In TB vaccination, our previous results demonstrated the advantages of *i.n.* immunization with Esx or PE/PPE antigens in various formulations (Dong et al., 2013; Sayes et al., 2016). Here, we characterized the functions and phenotypes of CD4<sup>+</sup> and CD8<sup>+</sup> T cells induced through systemic or *i.n.* administration of an optimized LV encoding EsxH or the HAEP(A) polyantigen. Importantly, the mucosal immunization was able to elicit lung CD4<sup>+</sup> and CD8<sup>+</sup> T cells having polyfunctional effector properties, accompanied by activated, tissue-resident, and memory pheno-

types. When formulated with cGAMP adjuvant and administered via *i.n.* instillation, the optimized LVs also triggered lung Th17 and Tc17 responses, which has prospective implications for the protection against Mtb (Counoupas et al., 2020; Desel et al., 2011; Shen and Chen, 2018; Van Dis et al., 2018). Whether the *i.n.* immunization involves the mediastinal lymph nodes and/or immune cells already located in or directly recruited from the blood to the lung parenchyma and whether organized ectopic lymphoid-like structures participate in the protection are questions that remain to be answered. These mucosal lymphoid structures, sometimes referred to as a “tertiary lymphoid organ,” mimic the immune germinal centers in tissues, providing local and controlled inflammation and creating an optimal environment for innate and adaptive immune cell cross talk to reinforce anti-microbial host immunity at sites of potential infection (Jones et al., 2016).

The very mild impact of LVs on DC maturation *in vitro* and the absence of major modifications in the lung innate immune cell composition following *i.n.* administration of LVs alone indicate the intrinsically low inflammatory properties of these vectors. Interestingly, DC signaling through IFN-I, *i.e.*, one of the rare inflammatory factors induced by LVs, is not involved in CD4<sup>+</sup> or CD8<sup>+</sup> T cell induction by these vectors. This suggests minimal involvement of innate immune pathways engaged by LVs in inducing robust T cell immunity. These characteristics, together with the non-replicative property of LVs, are promising indicators of safety for veterinary or human vaccinations, notably via the mucosal pathways. In addition, due to the mucosal barrier, *i.n.* immunization should generate minimal systemic adverse effects (Raeven et al., 2020). We observed that *in vitro* exposure of DCs to LVs induces very weak inflammatory responses but a significant IFN- $\alpha$  production. Even if not reproducible in all experimental settings, in some conditions, type I IFNs have been linked to TB disease severity (Moreira-Teixeira et al., 2018, 2020). However, *in vivo* administration of LVs induces only a low and transient (48 h) IFN- $\alpha$  response (Cousin et al., 2019), thus representing no threat for vaccine recipients in case of later encounter with Mtb.

One may wonder why the intensity of CD4<sup>+</sup> T cell responses seems weaker than that of CD8<sup>+</sup> T cell responses in mice immunized with LV::li. The ability of LVs to induce CD8<sup>+</sup> T cells is exceptional and this is probably why the levels of CD4<sup>+</sup> T cell responses appear to be relatively lower. In fact, if the levels of CD4<sup>+</sup> T cell responses induced by LV::li are compared with those induced by the good inducer of CD4<sup>+</sup> T cells, BCG (Sayes et al., 2016), it can be seen that the proportions of CD4<sup>+</sup> T cells detected by ICS in mice immunized with LV::li or BCG are comparable.

These data provide proof of concept that, in the context of LV, not only single small antigens, but also multiple antigens fused

control peptide. Shown are recapitulative total numbers of each (multi)functional population within the CD4<sup>+</sup> (A) or CD8<sup>+</sup> (B) T subsets located inside the parenchyma (CD45<sub>i.v.</sub><sup>-</sup>) or in the vasculature (CD45<sub>i.v.</sub><sup>+</sup>).

(C and D) Phenotyping of parenchymal (CD45<sub>i.v.</sub><sup>-</sup>) CD4<sup>+</sup> (C) or CD8<sup>+</sup> (D) T cells. Shown are representative dot plots for various T cells expressing various markers and recapitulative absolute numbers of each lung T cell subtype in individual mice.

Statistical significance was determined by two-tailed unpaired t test (\*\*p ≤ 0.001, \*\*\*\*p ≤ 0.0001). The experiment was performed twice: once with pooled cells inside each experimental group and once shown here, which was performed on cells recovered from individual mice.

See also Table S2.

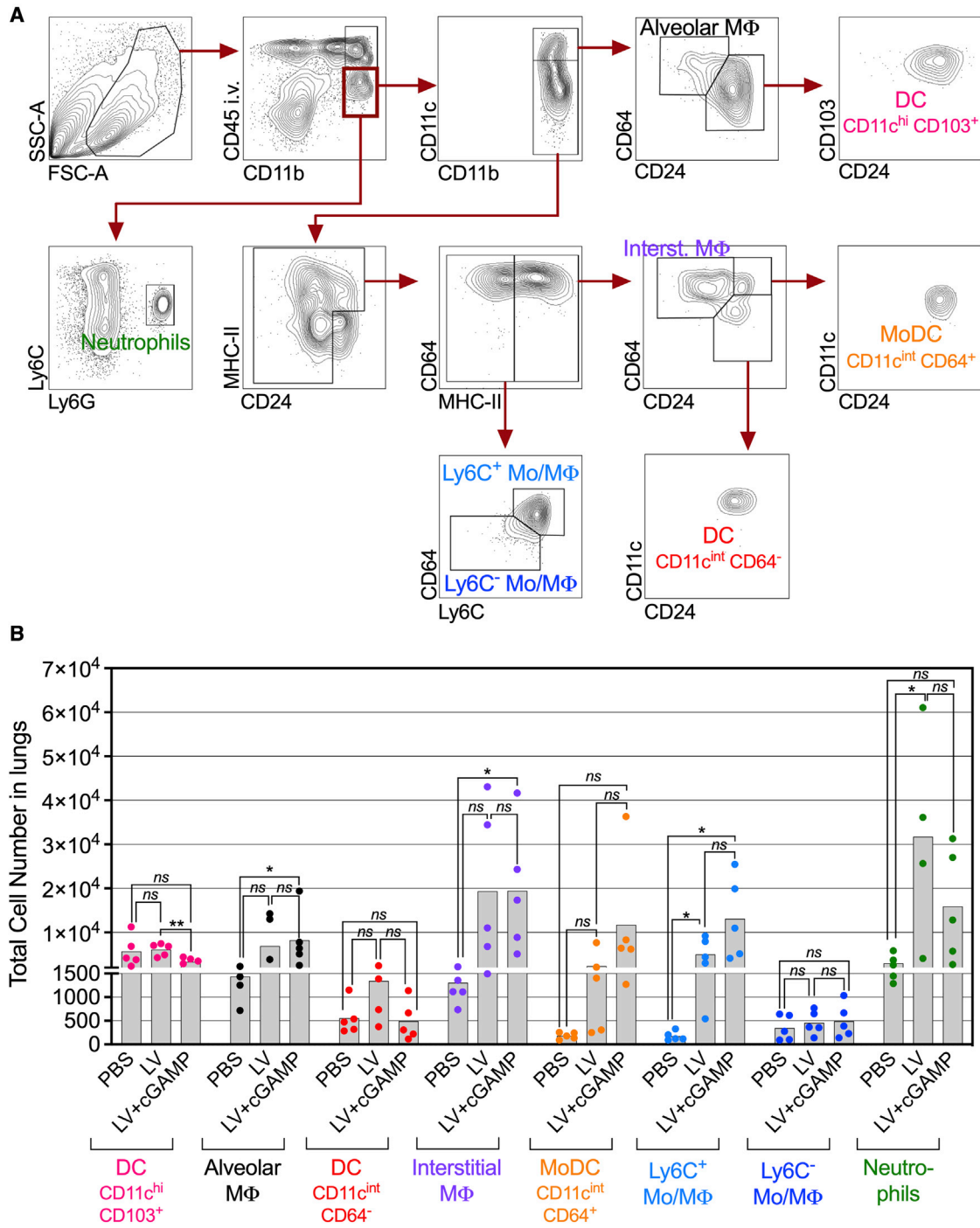


**Figure 5. Characterization of mucosal innate immune cell subsets in mice after LV i.n. administration**

C57BL/6 mice (n = 5/group) were immunized i.n. with  $5 \times 10^8$  TU of LV::li-EsxH alone or adjuvanted with cGAMP.

(A) At 1 dpi, after an i.v. injection of PE-anti-CD45 mAb 3 min before sacrifice, parenchymal innate immune cell subset cells (CD45<sup>i.v.</sup><sup>+</sup>) were detected. Cytometric gating strategy was used on CD11b<sup>+</sup> CD45<sup>i.v.</sup><sup>+</sup> cells to analyze various innate immune cell populations. Shown are cells from PBS-injected negative controls.

(B) Total cell numbers of each innate immune subset are indicated.

Statistical significance was determined by two-tailed unpaired t test (ns, not significant, \*p ≤ 0.05, \*\*p ≤ 0.01).

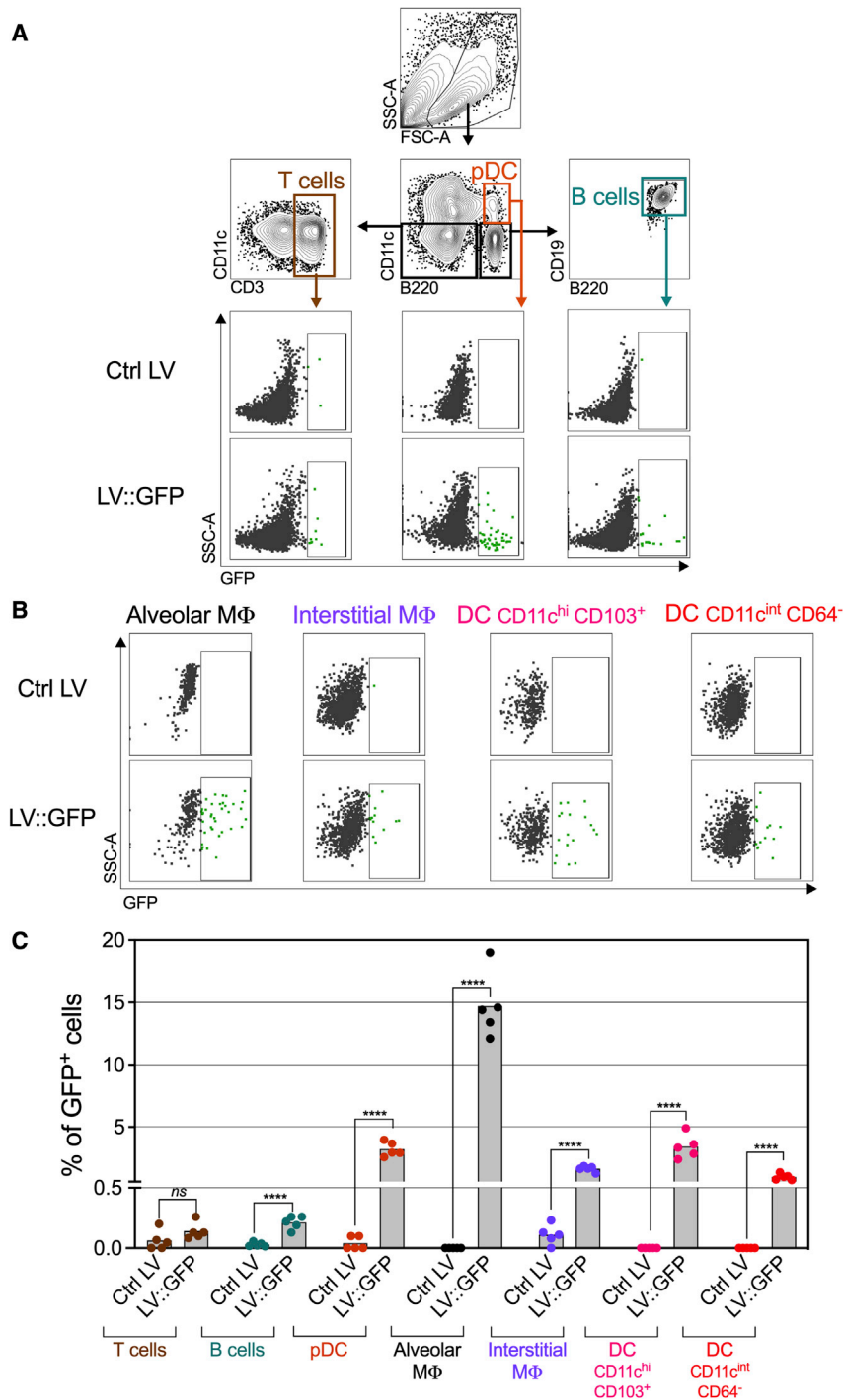


**Figure 6. Identification of cells transduced *in vivo* after i.n. administration**

C57BL/6 mice ( $n = 5/\text{group}$ ) were immunized i.n. with  $5 \times 10^8$  TU of LV::GFP or an empty LV (Ctrl LV), and the lungs were assessed individually 4 days later.

(A) Gating strategy and cytometric plots for detection of lung plasmacytoid DC (pDC) and T and B cells.

(B) The gating strategy to detect alveolar and interstitial macrophages, CD103<sup>+</sup> DCs, or CD11b<sup>+</sup> DC was the same as in (A).

(C) Percentages of GFP<sup>+</sup> cells inside each immune cell subset are indicated.

Statistical significance was evaluated by two-tailed unpaired t test (\*\*\*\* $p \leq 0.0001$ ).

adjuvantation of LV with cGAMP for use in i.n. immunization contributed to an influx/expansion of Ly6C<sup>+</sup> monocytes/macrophages, neutrophils, and natural killer (NK) cells, correlating with an increase in lung Th17 and Tc17 immunity. We showed a booster protective effect of LV::li-HAEP formulated in cGAMP in mice initially primed with BCG::ESX-1<sup>Mmar</sup> and a highly significant reduction of mycobacterial burden in the lungs and spleen of mice primed s.c. with LV::li-HAEP and boosted i.n. with cGAMP-adjuvanted LV::li-HAEP. Evaluation of the protective potential of LV::li-HAEP in Mtb post-exposure models will be also of interest in rodents.

Altogether, the non-replicative and very weakly inflammatory properties of LVs, now optimized to induce CD4<sup>+</sup> T cell responses, predict that these vectors could be tools of choice for mucosal vaccination, especially via the i.n. route. The prospects for development of these LV-based strategies go far beyond mycobacterial infections, extending the approach to acute or chronic respiratory infectious diseases.

#### Limitations of the study

One limitation of the strategy using fusion of li chain to antigenic fragments is that it will be difficult to include antigens longer than 450 amino acids at the risk of greatly reducing the efficiency of antigenic presentation

together, can gain access to the MHC-II presentation pathway, thanks to the addition of li to induce CD4<sup>+</sup> T cells, without reduction of CD8<sup>+</sup> T cell triggering. In addition, mucosal i.n. immunization with the optimized LVs induces recruitment and establishment of polyspecific lung CD4<sup>+</sup> and CD8<sup>+</sup> T cell immunity with resident-memory phenotype. This approach can optionally be improved by the addition of appropriate adjuvants. For instance,

by MHC-II. For this reason, we could not add the complete Ag85A sequence to the HAEP polyantigen, but only a single immunodominant epitope derived from this fifth selected Mtb antigen. Another limitation to the use of LVs in mass vaccinations in the field of infectious diseases is the challenging production of these vectors on an industrial scale and the cost of production, which remains quite high. However, we have now achieved a

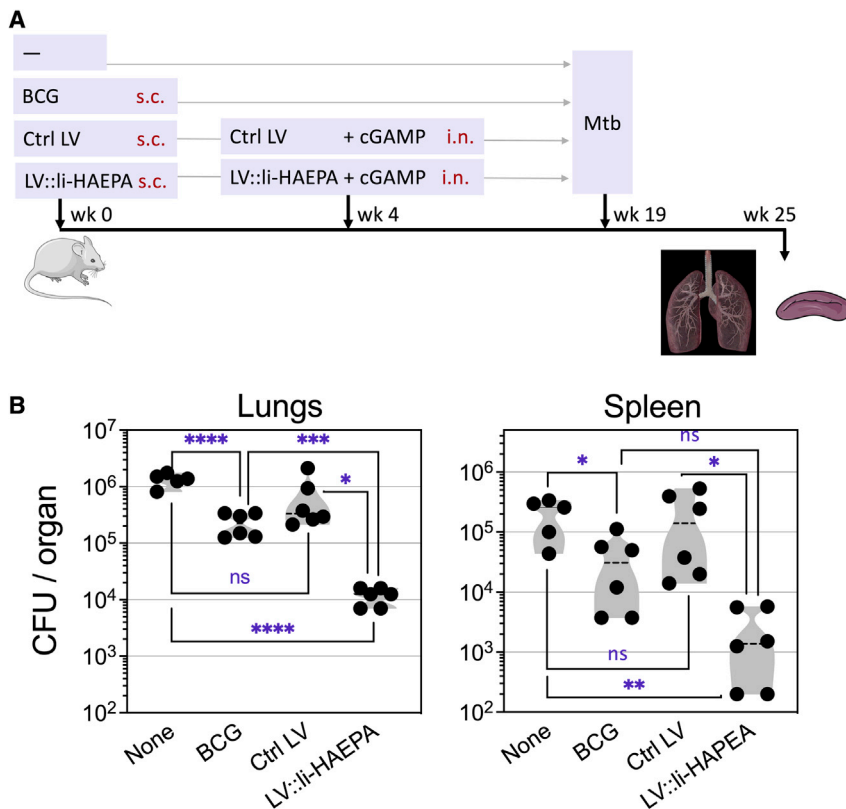


**Figure 7. Protective potential of LV::li-HAEPa in mice**

(A) Timeline of s.c. prime with LV::li-HAEPa and i.n. boost with cGAMP-adjuvanted LV::li-HAEPa and i.n. challenge with Mtb H37Rv strain, performed in C57BL/6 mice ( $n = 5-6/\text{group}$ ). Control mice received an empty LV (Ctrl LV). Control mice in other groups were immunized with BCG Pasteur alone or were left unvaccinated.

(B) Mycobacterial loads determined by CFU counting in the lungs and spleen of individual mice at week 6 post-challenge.

Statistical significance was determined by two-tailed unpaired t test (ns, not significant,  $*p \leq 0.05$ ,  $**p \leq 0.01$ ,  $***p \leq 0.001$ ,  $****p \leq 0.0001$ ).

See also Figures S7 and S8 and Table S3.

technology transfer to our industrial partners to enable the production of large quantities of LV-based vaccine candidates, which allows us to initiate several phase I clinical trials in prophylactic and therapeutic indications.

## STAR★METHODS

Detailed methods are provided in the online version of this paper and include the following:

- **KEY RESOURCES TABLE**
- **RESOURCE AVAILABILITY**
  - Lead contact
  - Materials availability
  - Data and code availability
- **EXPERIMENTAL MODEL AND SUBJECT DETAILS**
  - Mice, immunization
  - Protection assays
  - Mycobacteria
- **METHOD DETAILS**
  - Transfer LV plasmids encoding Mtb antigens
  - MHC-I or -II restricted antigen presentation
  - Intracellular cytokine staining
  - Lung cell phenotyping
  - Analysis of lung innate immune cells
  - Identification of LV-transduced lung cells
  - ELISPOT assay
  - Multiplex cytokine quantification assay

## ● QUANTIFICATION AND STATISTICAL ANALYSIS

### SUPPLEMENTAL INFORMATION

Supplemental information can be found online at <https://doi.org/10.1016/j.celrep.2022.111142>.

### ACKNOWLEDGMENTS

The authors are grateful to the late Dr. Florence Brossier (Hôpital Pitié-Salpêtrière, CNR-MyRMA, France) for providing the Mtb clinical isolates. This project received funding from the European Union's Horizon 2020 research and innovation program (TBVAC2020 643381) and the Marie Skłodowska-Curie grant agreement 665807. The work was also supported by the Programmes Transversaux de Recherche (PTR) 52-17 from the Institut Pasteur and in part by the French National Research Council ANR (ANR-10-LABX-62-IBEID) and the Institut Carnot Pasteur Microbes & Santé. M.-W.K. is a participant of the Pasteur-Paris University (PPU) International PhD Program.

### AUTHOR CONTRIBUTIONS

J.L., F.A., P.C., and L.M. conceived the study; J.L., P.A., A.P., M.-W.K., and L.M. performed experiments; C.B., P.S., F.M., and A.N. constructed and produced LVs and provided technical support; J.L., M.-W.K., P.C., and L.M. analyzed and interpreted data; D.H. and F.G. performed histology; W.S. and R.B. provided clinical isolates and live-attenuated vaccine; J.L., F.G., and L.M. wrote the manuscript; L.M. and P.C. secured funding.

### DECLARATION OF INTERESTS

P.C. is the founder and CSO of TheraVectys. J.L., F.A., P.A., M.-W.K., F.M., and A.N. are employees of TheraVectys. J.L., F.A., C.B., F.M., L.M., and

P.C. are inventors of a pending patent directed to LV immunization able to induce CD4<sup>+</sup> T cells.

Received: June 10, 2021

Revised: May 11, 2022

Accepted: June 7, 2022

Published: July 26, 2022

## REFERENCES

- Abdallah, A.M., Verboom, T., Weerdenburg, E.M., Gey van Pittius, N.C., Mahasha, P.W., Jiménez, C., Parra, M., Cadieux, N., Brennan, M.J., Appelmelk, B.J., and Bitter, W. (2009). PPE and PE\_PGRS proteins of *Mycobacterium marinum* are transported via the type VII secretion system ESX-5. *Mol. Microbiol.* **73**, 329–340.
- Allix-Béguec, C., Harmsen, D., Weniger, T., Supply, P., and Niemann, S. (2008). Evaluation and strategy for use of MIRU-VNTRplus, a multifunctional database for online analysis of genotyping data and phylogenetic identification of *Mycobacterium tuberculosis* complex isolates. *J. Clin. Microbiol.* **46**, 2692–2699.
- Andersen, P., and Scriba, T.J. (2019). Moving tuberculosis vaccines from theory to practice. *Nat. Rev. Immunol.* **19**, 550–562.
- Anderson, K.G., Mayer-Barber, K., Sung, H., Beura, L., James, B.R., Taylor, J.J., Qunaj, L., Griffith, T.S., Vezys, V., Barber, D.L., and Masopust, D. (2014). Intravascular staining for discrimination of vascular and tissue leukocytes. *Nat. Protoc.* **9**, 209–222.
- Arhel, N.J., Souquere-Besse, S., Munier, S., Souque, P., Guadagnini, S., Ruthersford, S., Prévost, M.C., Allen, T.D., and Charneau, P. (2007). HIV-1 DNA Flap formation promotes uncoating of the pre-integration complex at the nuclear pore. *EMBO J.* **26**, 3025–3037.
- Banu, S., Honoré, N., Saint-Joanis, B., Philpott, D., Prévost, M.C., and Cole, S.T. (2002). Are the PE-PGRS proteins of *Mycobacterium tuberculosis* variable surface antigens? *Mol. Microbiol.* **44**, 9–19.
- Brown, B.D., Sitia, G., Annoni, A., Hauben, E., Sergi, L.S., Zingale, A., Roncarolo, M.G., Guidotti, L.G., and Naldini, L. (2007). In vivo administration of lentiviral vectors triggers a type I interferon response that restricts hepatocyte gene transfer and promotes vector clearance. *Blood* **109**, 2797–2805.
- Bull, N.C., Stylianou, E., Kaveh, D.A., Pinpathomrat, N., Pasricha, J., Harrington-Kandt, R., Garcia-Pelayo, M.C., Hogarth, P.J., and McShane, H. (2019). Enhanced protection conferred by mucosal BCG vaccination associates with presence of antigen-specific lung tissue-resident PD-1(+) KLRG1(-) CD4(+) T cells. *Mucosal Immunol.* **12**, 555–564.
- Capone, S., Naddeo, M., D'Alise, A.M., Abbate, A., Grazioli, F., Del Gaudio, A., Del Sorbo, M., Esposito, M.L., Ammendola, V., Perretta, G., et al. (2014). Fusion of HCV nonstructural antigen to MHC class II-associated invariant chain enhances T-cell responses induced by vectored vaccines in nonhuman primates. *Mol. Ther.* **22**, 1039–1047.
- Caton, M.L., Smith-Raska, M.R., and Reizis, B. (2007). Notch-RBP-J signaling controls the homeostasis of CD8<sup>-</sup> dendritic cells in the spleen. *J. Exp. Med.* **204**, 1653–1664.
- Chiu, C., and Openshaw, P.J. (2015). Antiviral B cell and T cell immunity in the lungs. *Nat. Immunol.* **16**, 18–26.
- Cole, S.T., Brosch, R., Parkhill, J., Garnier, T., Churcher, C., Harris, D., Gordon, S.V., Eiglmeier, K., Gas, S., Barry, C.E., 3rd., et al. (1998). Deciphering the biology of *Mycobacterium tuberculosis* from the complete genome sequence. *Nature* **393**, 537–544.
- Counoupas, C., Ferrell, K.C., Ashhurst, A., Bhattacharyya, N.D., Nagalingam, G., Stewart, E.L., Feng, C.G., Petrovsky, N., Britton, W.J., and Triccas, J.A. (2020). Mucosal delivery of a multistage subunit vaccine promotes development of lung-resident memory T cells and affords interleukin-17-dependent protection against pulmonary tuberculosis. *NPJ Vaccines* **5**, 105.
- Cousin, C., Oberkamp, M., Felix, T., Rosenbaum, P., Weil, R., Fabrega, S., Morante, V., Negri, D., Cara, A., Dadaglio, G., and Leclerc, C. (2019). Persistence of integrase-deficient lentiviral vectors correlates with the induction of STING-independent CD8(+) T cell responses. *Cell Rep.* **26**, 1242–1257.e7.
- Cresswell, P., and Roche, P.A. (2014). Invariant chain-MHC class II complexes: always odd and never invariant. *Immunol. Cell Biol.* **92**, 471–472.
- D'Souza, S., Rosseels, V., Romano, M., Tanghe, A., Denis, O., Jurion, F., Castiglione, N., Vanonckelen, A., Palfliet, K., and Huygen, K. (2003). Mapping of murine Th1 helper T-Cell epitopes of mycolyl transferases Ag85A, Ag85B, and Ag85C from *Mycobacterium tuberculosis*. *Infect. Immun.* **71**, 483–493.
- Desel, C., Dorhoi, A., Bandermann, S., Grode, L., Eisele, B., and Kaufmann, S.H.E. (2011). Recombinant BCG DeltaureC hly+ induces superior protection over parental BCG by stimulating a balanced combination of type 1 and type 17 cytokine responses. *J. Infect. Dis.* **204**, 1573–1584.
- Dhatchinamoorthy, K., Colbert, J.D., and Rock, K.L. (2021). Cancer immune evasion through loss of MHC class I antigen presentation. *Front. Immunol.* **12**, 636568.
- Di Nunzio, F., Félix, T., Arhel, N.J., Nisole, S., Charneau, P., and Beignon, A.S. (2012). HIV-derived vectors for therapy and vaccination against HIV. *Vaccine* **30**, 2499–2509.
- Diebold, S.S., Cotten, M., Koch, N., and Zenke, M. (2001). MHC class II presentation of endogenously expressed antigens by transfected dendritic cells. *Gene Ther.* **8**, 487–493.
- Dong, H., Stanek, O., Salvador, F.R., Länger, U., Morillon, E., Ung, C., Sebo, P., Leclerc, C., and Majlessi, L. (2013). Induction of protective immunity against *Mycobacterium tuberculosis* by delivery of ESX antigens into airway dendritic cells. *Mucosal Immunol.* **6**, 522–534.
- Esposito, I., Cicconi, P., D'Alise, A.M., Brown, A., Esposito, M., Swadling, L., Holst, P.J., Bassi, M.R., Stornauiolo, M., Mori, F., et al. (2020). MHC class II invariant chain-adjuvanted viral vectored vaccines enhances T cell responses in humans. *Sci. Transl. Med.* **12**, eaaz7715.
- Esslinger, C., Romero, P., and MacDonald, H.R. (2002). Efficient transduction of dendritic cells and induction of a T-cell response by third-generation lentivectors. *Hum. Gene Ther.* **13**, 1091–1100.
- Flórido, M., Mufflihah, H., Lin, L.C.W., Xia, Y., Siero, F., Palendira, M., Feng, C.G., Bertolino, P., Stambas, J., Triccas, J.A., and Britton, W.J. (2018). Pulmonary immunization with a recombinant influenza A virus vaccine induces lung-resident CD4(+) memory T cells that are associated with protection against tuberculosis. *Mucosal Immunol.* **11**, 1743–1752.
- Gagneux, S. (2018). Ecology and evolution of *Mycobacterium tuberculosis*. *Nat. Rev. Microbiol.* **16**, 202–213.
- Gröschel, M.I., Sayes, F., Shin, S.J., Frigui, W., Pawlik, A., Orgeur, M., Canetti, R., Honoré, N., Simeone, R., van der Werf, T.S., et al. (2017). Recombinant BCG expressing ESX-1 of *Mycobacterium marinum* combines low virulence with cytosolic immune signaling and improved TB protection. *Cell Rep.* **18**, 2752–2765.
- Gröschel, M.I., Sayes, F., Simeone, R., Majlessi, L., and Brosch, R. (2016). ESX secretion systems: mycobacterial evolution to counter host immunity. *Nat. Rev. Microbiol.* **14**, 677–691.
- Hastie, E., Cataldi, M., Marriott, I., and Grdzelskivili, V.Z. (2013). Understanding and altering cell tropism of vesicular stomatitis virus. *Virus Res.* **176**, 16–32.
- He, Y., Zhang, J., Mi, Z., Robbins, P., and Falo, L.D., Jr. (2005). Immunization with lentiviral vector-transduced dendritic cells induces strong and long-lasting T cell responses and therapeutic immunity. *J. Immunol.* **174**, 3808–3817.
- Hervas-Stubbs, S., Majlessi, L., Simsova, M., Morova, J., Rojas, M.J., Nouzé, C., Brodin, P., Sebo, P., and Leclerc, C. (2006). High frequency of CD4<sup>+</sup> T cells specific for the TB10.4 protein correlates with protection against *Mycobacterium tuberculosis* infection. *Infect. Immun.* **74**, 3396–3407.
- Holmgren, J., and Czerkinsky, C. (2005). Mucosal immunity and vaccines. *Nat. Med.* **11**, S45–S53.
- Hu, B., Tai, A., and Wang, P. (2011). Immunization delivered by lentiviral vectors for cancer and infectious diseases. *Immunol. Rev.* **239**, 45–61.

- Iantomasi, R., Sali, M., Cascioferro, A., Palucci, I., Zumbo, A., Soldini, S., Rocca, S., Greco, E., Maulucci, G., De Spirito, M., et al. (2012). PE\_PGRS30 is required for the full virulence of *Mycobacterium tuberculosis*. *Cell Microbiol.* **14**, 356–367. <https://doi.org/10.1111/j.1462-5822>.
- Jones, G.W., Hill, D.G., and Jones, S.A. (2016). Understanding immune cells in tertiary lymphoid organ development: it is all starting to come together. *Front. Immunol.* **7**, 401.
- Kreiter, S., Selmi, A., Diken, M., Sebastian, M., Osterloh, P., Schild, H., Huber, C., Türeci, O., and Sahin, U. (2008). Increased antigen presentation efficiency by coupling antigens to MHC class I trafficking signals. *J. Immunol.* **180**, 309–318.
- Ku, M.W., Anna, F., Souque, P., Petres, S., Prot, M., Simon-Loriere, E., Charneau, P., and Bourguine, M. (2020). A single dose of NILV-based vaccine provides rapid and durable protection against Zika virus. *Mol. Ther.* **28**, 1772–1782.
- Ku, M.W., Authié, P., Bourguine, M., Anna, F., Noirat, A., Moncoq, F., Vesin, B., Nevo, F., Lopez, J., Souque, P., et al. (2021a). Full brain and lung prophylaxis against SARS-CoV-2 by intranasal lentiviral vaccination in a new hACE2 transgenic mouse model or golden hamsters. Preprint at bioRxiv. <https://doi.org/10.1101/2021.02.03.429211>.
- Ku, M.W., Authié, P., Bourguine, M., Anna, F., Noirat, A., Moncoq, F., Vesin, B., Nevo, F., Lopez, J., Souque, P., et al. (2021b). Brain cross-protection against SARS-CoV-2 variants by a lentiviral vaccine in new transgenic mice. *EMBO Mol. Med.* **13**, e14459.
- Ku, M.W., Authié, P., Nevo, F., Souque, P., Bourguine, M., Romano, M., Charneau, P., and Majlessi, L. (2021c). Lentiviral vector induces high-quality memory T cells via dendritic cells transduction. *Commun. Biol.* **4**, 713.
- Ku, M.W., Bourguine, M., Authié, P., Lopez, J., Nemirov, K., Moncoq, F., Noirat, A., Vesin, B., Nevo, F., Blanc, C., et al. (2021d). Intranasal vaccination with a lentiviral vector protects against SARS-CoV-2 in preclinical animal models. *Cell Host Microbe* **29**, 236–249.e6.
- Ku, M.W., Charneau, P., and Majlessi, L. (2021e). Use of lentiviral vectors in vaccination. *Expert Rev. Vaccines* **20**, 1571–1586.
- Le Bon, A., Thompson, C., Kamphuis, E., Durand, V., Rossmann, C., Kalinke, U., and Tough, D.F. (2006). Cutting edge: enhancement of antibody responses through direct stimulation of B and T cells by type I IFN. *J. Immunol.* **176**, 2074–2078.
- Lewinsohn, D.A., Lewinsohn, D.M., and Scriba, T.J. (2017). Polyfunctional CD4<sup>+</sup> T cells as targets for tuberculosis vaccination. *Front. Immunol.* **8**, 1262.
- Liechtenstein, T., Dufait, I., Bricogne, C., Lanna, A., Pen, J., Breckpot, K., and Escors, D. (2012). PD-L1/PD-1 Co-stimulation, a brake for T cell activation and a T cell differentiation signal. *J. Clin. Cell. Immunol.* **S12**, 006.
- Lindestam Arlehamn, C.S., Gerasimova, A., Mele, F., Henderson, R., Swann, J., Greenbaum, J.A., Kim, Y., Sidney, J., James, E.A., Taplitz, R., et al. (2013). Memory T cells in latent *Mycobacterium tuberculosis* infection are directed against three antigenic islands and largely contained in a CXCR3+CCR6+ Th1 subset. *PLoS Pathog.* **9**, e1003130.
- Majlessi, L., and Charneau, P. (2021). [An anti-Covid-19 lentiviral vaccine candidate that can be administered by the nasal route]. *Med. Sci.* **37**, 1172–1175.
- Majlessi, L., Prados-Rosales, R., Casadevall, A., and Brosch, R. (2015). Release of mycobacterial antigens. *Immunol. Rev.* **264**, 25–45.
- Majlessi, L., Rojas, M.J., Brodin, P., and Leclerc, C. (2003). CD8<sup>+</sup>-T-cell responses of *Mycobacterium*-infected mice to a newly identified major histocompatibility complex class I-restricted epitope shared by proteins of the ESAT-6 family. *Infect. Immun.* **71**, 7173–7177.
- Mensali, N., Grenov, A., Pati, N.B., Dillard, P., Myhre, M.R., Gaudernack, G., Kvalheim, G., Inderberg, E.M., Bakke, O., and Wälchli, S. (2019). Antigen-delivery through invariant chain (CD74) boosts CD8 and CD4 T cell immunity. *Oncoimmunology* **8**, 1558663.
- Moreira-Teixeira, L., Mayer-Barber, K., Sher, A., and O'Garra, A. (2018). Type I interferons in tuberculosis: foe and occasionally friend. *J. Exp. Med.* **215**, 1273–1285.
- Moreira-Teixeira, L., Stimpson, P.J., Stavropoulos, E., Hadebe, S., Chakravarty, P., Ioannou, M., Aramburu, I.V., Herbert, E., Priestnall, S.L., Suarez-Bonet, A., et al. (2020). Type I IFN exacerbates disease in tuberculosis-susceptible mice by inducing neutrophil-mediated lung inflammation and NETosis. *Nat. Commun.* **11**, 5566.
- Mueller, S.N., and Mackay, L.K. (2016). Tissue-resident memory T cells: local specialists in immune defence. *Nat. Rev. Immunol.* **16**, 79–89.
- Park, C.O., and Kupper, T.S. (2015). The emerging role of resident memory T cells in protective immunity and inflammatory disease. *Nat. Med.* **21**, 688–697.
- Perdomo, C., Zedler, U., Kuhl, A.A., Lozza, L., Saikali, P., Sander, L.E., Vogelzang, A., Kaufmann, S.H., and Kupz, A. (2016). Mucosal BCG vaccination induces protective lung-resident memory T cell populations against tuberculosis. *mBio* **7**, e01686-16.
- Pichlmair, A., Diebold, S.S., Gschmeissner, S., Takeuchi, Y., Ikeda, Y., Collins, M.K., and Reis e Sousa, C. (2007). Tubulovesicular structures within vesicular stomatitis virus G protein-pseudotyped lentiviral vector preparations carry DNA and stimulate antiviral responses via Toll-like receptor 9. *J. Virol.* **81**, 539–547.
- Raeven, R.H.M., Rockx-Brouwer, D., Kanojia, G., van der Maas, L., Bindels, T.H.E., Ten Have, R., van Riet, E., Metz, B., and Kersten, G.F.A. (2020). Intranasal immunization with outer membrane vesicle pertussis vaccine confers broad protection through mucosal IgA and Th17 responses. *Sci. Rep.* **10**, 7396.
- Rowe, H.M., Lopes, L., Ikeda, Y., Bailey, R., Barde, I., Zenke, M., Chain, B.M., and Collins, M.K. (2006). Immunization with a lentiviral vector stimulates both CD4 and CD8 T cell responses to an ovalbumin transgene. *Mol. Ther.* **13**, 310–319.
- Sakai, S., Kauffman, K.D., Schenkel, J.M., McBerry, C.C., Mayer-Barber, K.D., Masopust, D., and Barber, D.L. (2014). Cutting edge: control of *Mycobacterium tuberculosis* infection by a subset of lung parenchyma-homing CD4 T cells. *J. Immunol.* **192**, 2965–2969.
- Sayes, F., Blanc, C., Ates, L.S., Deboosere, N., Orgeur, M., Le Chevalier, F., Gröschel, M.I., Frigui, W., Song, O.R., Lo-Man, R., et al. (2018). Multiplexed quantitation of intraphagocyte *Mycobacterium tuberculosis* secreted protein effectors. *Cell Rep.* **23**, 1072–1084.
- Sayes, F., Pawlik, A., Frigui, W., Gröschel, M.I., Crommelynck, S., Fayolle, C., Cia, F., Bancroft, G.J., Bottai, D., Leclerc, C., et al. (2016). CD4<sup>+</sup> T cells recognizing PE/PPE antigens directly or via cross reactivity are protective against pulmonary *Mycobacterium tuberculosis* infection. *PLoS Pathog.* **12**, e1005770.
- Sayes, F., Sun, L., Di Luca, M., Simeone, R., Degaiffier, N., Fiette, L., Esin, S., Brosch, R., Bottai, D., Leclerc, C., and Majlessi, L. (2012). Strong immunogenicity and cross-reactivity of *Mycobacterium tuberculosis* ESX-5 type VII secretion: encoded PE-PPE proteins predicts vaccine potential. *Cell Host Microbe* **11**, 352–363.
- Schenkel, J.M., and Masopust, D. (2014). Tissue-resident memory T cells. *Immunity* **41**, 886–897.
- Shen, H., and Chen, Z.W. (2018). The crucial roles of Th17-related cytokines/signal pathways in *M. tuberculosis* infection. *Cell. Mol. Immunol.* **15**, 216–225.
- Shepherd, F.R., and McLaren, J.E. (2020). T cell immunity to bacterial pathogens: mechanisms of immune control and bacterial evasion. *Int. J. Mol. Sci.* **21**, E6144.
- Sirven, A., Pflumio, F., Zennou, V., Titeux, M., Vainchenker, W., Coulombel, L., Dubart-Kupperschmitt, A., and Charneau, P. (2000). The human immunodeficiency virus type-1 central DNA flap is a crucial determinant for lentiviral vector nuclear import and gene transduction of human hematopoietic stem cells. *Blood* **96**, 4103–4110.
- Turner, D.L., Bickham, K.L., Thome, J.J., Kim, C.Y., D'Ovidio, F., Wherry, E.J., and Farber, D.L. (2014). Lung niches for the generation and maintenance of tissue-resident memory T cells. *Mucosal Immunol.* **7**, 501–510.
- Van Dis, E., Sogi, K.M., Rae, C.S., Sivick, K.E., Surh, N.H., Leong, M.L., Kanne, D.B., Metchette, K., Leong, J.J., Brumfiel, J.R., et al. (2018). STING-activating

adjuvants elicit a Th17 immune response and protect against Mycobacterium tuberculosis infection. *Cell Rep.* 23, 1435–1447.

Vesin, B., Lopez, J., Noirat, A., Authié, P., Fert, I., Le Chevalier, F., Moncoq, F., Nemirov, K., Blanc, C., Planchais, C., et al. (2022). An intranasal lentiviral booster reinforces the waning mRNA vaccine-induced SARS-CoV-2 immunity that it targets to lung mucosa. *Mol. Ther.* <https://doi.org/10.1016/j.ymthe.2022.04.016>.

Zennou, V., Petit, C., Guetard, D., Nerhbass, U., Montagnier, L., and Charneau, P. (2000). HIV-1 genome nuclear import is mediated by a central DNA flap. *Cell* 101, 173–185.

Zennou, V., Serguera, C., Sarkis, C., Colin, P., Perret, E., Mallet, J., and Charneau, P. (2001). The HIV-1 DNA flap stimulates HIV vector-mediated cell transduction in the brain. *Nat. Biotechnol.* 19, 446–450.

STAR★METHODS

KEY RESOURCES TABLE

REAGENT or RESOURCE	SOURCE	IDENTIFIER
<b>Antibodies</b>		
anti-CD28 (clone 37.51)	BD Biosciences	Cat# 553294 RRID: AB_394763
anti-CD49d (clone 9C10-MFR4.B)	BD Biosciences	Cat# 553313 RRID: AB_394776
PE-Cy7-anti-CD107a (clone 1D4B)	BioLegend	Cat# 121620 RRID: AB_2562147
PerCP-Cy5.5-anti-CD3e (clone 145-2C11) eBioscience™	Thermo Fisher Scientific	Cat# 45-0031-82 RRID: AB_1107000
PE-Cy7-anti-CD4 (clone RM4-5)	BD Biosciences	Cat# 552775 RRID: AB_394461
BV711-anti-CD8 (clone 53-6.7)	BD Biosciences	Cat# 563046 RRID: AB_2737972
BV421-anti-IL-2 (clone JES6-5H4)	BD Biosciences	Cat# 562969 RRID: AB_2737923
FITC-anti-TNF (MP6-XT22),	BD Biosciences	Cat# 554418 RRID: AB_395379
APC-anti-IFN- $\gamma$ (clone XMG1.2)	BD Biosciences	Cat# 554413 RRID: AB_398551
BV605-anti-IL-17A (Clone TC11-18H10)	BD Biosciences	Cat# 564169 RRID: AB_2738640
PE-anti-CD45 (clone 30-F11)	BioLegend	Cat# 103106 RRID: AB_312971
BV650-anti-CD3e (clone 145-2C11)	BD Biosciences	Cat# 564378 RRID: AB_2738779
eF450-anti-CD4 (clone RM4-5) eBioscience™	Thermo Fisher Scientific	Cat# 48-0042-82 RRID: AB_1272194)
APC-anti-CD8 (clone 53-6.7) eBioscience™	Thermo Fisher Scientific	Cat# 17-0081-82 RRID: AB_469335
PE-Cy7-anti-CD27 (clone LG.7F9) eBioscience™	Thermo Fisher Scientific	Cat# 25-0271-80 RRID: AB_1724037
AF700-anti-CD62L (clone MEL-14)	BD Biosciences	Cat# 560517 RRID: AB_1645210
BV605-anti-CD69 (clone H1.2F3)	BioLegend	Cat# 104529 RRID: AB_11203710
BV711-anti-CD103 (clone 2E7)	BioLegend	Cat# 121435 RRID: AB_2686970
AF700-anti-CD44 (clone IM7)	BioLegend	Cat# 103025 RRID: AB_493712
FITC-anti-CXCR3 (clone CXCR3-173) eBioscience™	Thermo Fisher Scientific	Cat# 11-1831-82 RRID: AB_11040010
APC-anti-CD11b (clone M1/70)	BD Biosciences	Cat# 553312 RRID: AB_398535
PE-Cy7-anti-CD11c (clone N418) eBioscience™	Thermo Fisher Scientific	Cat# 25-0114-81 RRID: AB_469589
BV421-anti-CD64 (clone X54-5/7.1)	Biolegend	Cat# 139309 RRID: AB_2562694

(Continued on next page)

REAGENT or RESOURCE	SOURCE	IDENTIFIER
FITC-anti-CD24 (clone M1/69)	BD Biosciences	Cat# 561777 RRID: AB_10896486
PerCP-Cy5.5-anti-MHC-II (clone M5/114)	BD Biosciences	Cat# 562363 RRID: AB_11153297
FITC-anti-Ly6G (clone 1A8)	Biologend	Cat# 127605 RRID: AB_1236488
BV605-anti- Ly6C (clone HK1.4)	Biologend	Cat# 128035 RRID: AB_2562352
BV605-anti-CD45 (clone 30-F11)	BD Biosciences	Cat# 563053 RRID: AB_2737976
PE-anti-CD11b (clone M1/70) eBioscience™	Thermo Fisher Scientific	Cat# 12-0112-81 RRID: AB_465546
APC-anti-CD11c (clone N418)	Miltenyi Biotec	Cat# 130-110-702 RRID: AB_2654710
PE-Cy7-anti-CD24 (clone M1/69)	Biologend	Cat# 101821 RRID: AB_756047
eF450-anti-CD19 (clone 1D3) eBioscience™	Thermo Fisher Scientific	Cat# 48-0193-82 RRID: AB_2734905
PE-anti-B220 (clone REA755)	Miltenyi Biotec	Cat# 130-110-709 RRID: AB_2658276
FcγII/III receptor blocking anti-CD16/CD32 (clone 2.4G2)	BD Biosciences	Cat# 553140 RRID: AB_394655
Near IR Live/Dead	Invitrogen	Cat# L34976 N/A
<b>Bacterial and virus strains</b>		
<i>Mycobacterium tuberculosis</i> clinical isolates (See Table S3)	This paper	N/A
BCG::ESX-1 <sup>Mmar</sup>	<a href="#">Groschel et al., 2017</a>	N/A
LV::EsxH	This paper	N/A
LV::li-EsxH	This paper	N/A
LV::TfR <sub>1-118</sub> -EsxH	This paper	N/A
LV::SP-EsxH-MITD	This paper	N/A
LV::OVA	This paper	N/A
LV::li-HAEP	This paper	N/A
LV::li-HAEP A	This paper	N/A
LV::empty	This paper	N/A
LV::GFP	<a href="#">Zennou et al., 2000</a>	<a href="https://doi.org/10.1016/S0092-8674(00)80828-4">https://doi.org/10.1016/S0092-8674(00)80828-4</a>
<b>Chemicals, peptides, and recombinant proteins</b>		
EsxH: 20-28 peptide	ProteoGenix	N/A
EsxH: 74-88 peptide	ProteoGenix	N/A
EsxA: 1-20 peptide	ProteoGenix	N/A
PE19: 1-18 peptide	ProteoGenix	N/A
EspC:40-54 peptide	ProteoGenix	N/A
Ag85A:241-260 peptide	ProteoGenix	N/A
<b>Critical commercial assays</b>		
Fixation/Permeabilization Solution Kit with BD GolgiPlug™	BD Biosciences	Cat# 555028 RRID: AB_2869013
BD GolgiStop™	BD Biosciences	Cat# 554724 N/A
BD Cytotfix	BD Biosciences	Cat# 554655 NA

(Continued on next page)

**Continued**

REAGENT or RESOURCE	SOURCE	IDENTIFIER
Mouse IFN- $\gamma$ ELISPOT <sup>PLUS</sup>	Mabtech	Cat# 3321-4APW N/A
Mouse TNF ELISPOT <sup>PLUS</sup>	Mabtech	Cat# 3511-4APW N/A

Experimental models: Cell lines

HEK293T cells	ATCC	HEK293T cells
T-cell hybridoma specific to EsxH: 20-28 (YB8)	<a href="#">Majlessi et al., 2003</a>	N/A
T-cell hybridoma specific to EsxH: 74-88 (1H2)	<a href="#">Hervas-Stubbs et al., 2006</a>	N/A
T-cell hybridoma specific to EsxA: 1-20 (NB11)	<a href="#">Hervas-Stubbs et al., 2006</a>	N/A
T-cell hybridoma specific to PE19: 1-18 (IF6)	<a href="#">Sayes et al., 2018</a>	N/A
T-cell hybridoma specific to Ag85A:241-260 (DE10)	<a href="#">Majlessi et al., 2003</a>	N/A

Experimental models: Organisms/strains

Mouse: C57BL/6J	Janvier, Le Genest Saint Isle, France	Cat# SC-C57J-F N/A
Mouse: BALB/c	Janvier, Le Genest Saint Isle, France	Cat# SC-BALBJ-F N/A
<i>ifnar1<sup>fllox/fllox</sup></i> pCD11c-Cre <sup>+</sup>	This paper	N/A

Oligonucleotides

Titration of LV: Forward 5'-TGGAGGAGGA GATATGAGGG-3' Reverse 5'-CTG CTG CAC TAT ACC AGA CA-3' specific to pFLAP plasmid Forward 5'-TCTCTCTGACTTCA ACAGC-3' and Reverse 5'-CCCTG CACTTTTAAAGAGCC-3' specific to <i>gadh</i> gene	This paper	N/A
--	------------	-----

Recombinant DNA

pFlap-ieCMV-WPREm	<a href="#">Zennou et al., 2000</a>	<a href="https://doi.org/10.1016/S0092-8674(00)80828-4">https://doi.org/10.1016/S0092-8674(00)80828-4</a>
pFlap-SP1-B2m-EsxH-WPREm	This paper	N/A
pFlap-SP1-B2m-mli-EsxH-WPREm	This paper	N/A
pFlap-SP1-B2m-TfR <sub>1-118</sub> -EsxH-WPREm	This paper	N/A
pFlap-SP1-B2m-SP-EsxH-MITD-WPREm	This paper	N/A
pFlap-SP1-B2m-li-HAPE-WPREm	This paper	N/A
pFlap-SP1-B2m-li-HAPEA-WPREm	This paper	N/A

Software and algorithms

GraphPad Prism	GraphPad	v 9.0.0
FlowJo	FlowJo LLC	v10

**RESOURCE AVAILABILITY**

**Lead contact**

Further information and requests for resources and reagents should be directed to and will be fulfilled by the lead contact, Laleh Majlessi ([laleh.majlessi@pasteur.fr](mailto:laleh.majlessi@pasteur.fr)).

### Materials availability

Plasmids generated in this study have been deposited to “La Collection Nationale de Cultures de Microorganismes” (CNCM), Institut Pasteur. All plasmids and LV generated in this study will be available under MTA for research use, given a pending patent directed to an LV::li vaccination vectors.

### Data and code availability

- The published article includes all datasets generated and analyzed during this study. Any additional information required to re-analyze the data reported in this paper is available from the [lead contact](#) upon request.
- This paper does not report original code.

## EXPERIMENTAL MODEL AND SUBJECT DETAILS

### Mice, immunization

Female BALB/c (H-2<sup>d</sup>) and C57BL/6 (H-2<sup>b</sup>) (Janvier Labs, Le Genest-Saint-Isle, France) were immunized after at least one week of acclimatation, with the indicated dose of LV contained in 50  $\mu$ L/mouse for i.m. injection, in 200  $\mu$ L/mouse for s.c. at the basis of the tail, or in 20  $\mu$ L/mouse for i.n. instillation. The i.n. administration was performed under general anesthesia, obtained by i.p. injection of 100  $\mu$ L of PBS containing weight-adapted quantities of Imalgène<sub>1,000</sub> (Kétamine, i.e., 100 mg/kg, Merial, France) and Rompun 2% (Xylazine solution, 10 mg/kg, Bayer, Germany). When indicated LV was adjuvanted with 10  $\mu$ g/mouse of cGAMP (Invivogen).

The hemizygous C57BL/6 (H-2<sup>b</sup>) mice, carrying the gene encoding Cre DNA recombinase, under the regulation of murine CD11c promoter (Caton et al., 2007), were crossed with C57BL/6 mice homozygous for the “floxed” *ifnar1* allele (Le Bon et al., 2006) to obtain litters of homozygous *ifnar1*<sup>flox/flox</sup> mice that carry or not the Cre transgene. In *ifnar1*<sup>flox/flox</sup> pCD11c-Cre<sup>+</sup> mice, with the exception of CD11c-expressing plasmacytoid DC, all other DC populations lacked IFNAR1 (Le Bon et al., 2006). The breeding was performed at the central animal facilities of Institut Pasteur, under SPF conditions.

Only female mice were used, between the age of 8 and 16 weeks, in accordance with the European and French directives (Directive 86/609/CEE and Decree 87–848 of 19 October 1987), after approval by the Institut Pasteur Safety, Animal Care and Use Committee, under local ethical committee protocol agreement # CETEA 2013–0036, CETEA dap180023) and CETEA 2012–0005 (APA-FIS#14638-2018041214002048).

### Protection assays

Female C57BL/6 mice were primed s.c. with  $1 \times 10^6$  CFU/mouse of BCG::ESX-1<sup>Mmar</sup> (Groschel et al., 2017) at day 0, boosted s.c. with  $5 \times 10^8$  TU/mouse of adjuvanted LV at week 5, and boosted again i.n. with  $5 \times 10^8$  TU/mouse of adjuvanted LV at week 10. The immunized mice, as well as age-matched, unvaccinated controls, were challenged 2 weeks after the i.n. boost by use of a homemade nebulizer via aerosol, as previously described (Sayes et al., 2016). Briefly, 5 mL of a suspension of  $1.7 \times 10^6$  CFU/mL of H37Rv Mtb strain were aerosolized to deliver an inhaled dose of  $\approx 200$  CFU/mouse. The infected mice were placed in isolator in BSL3 facilities at Institut Pasteur. Five weeks later, lungs or spleen of the infected mice were homogenized by using a MillMixer homogenizer (Qiagen, Courtaboeuf, France) and serial 5-fold dilutions prepared in PBS were plated on 7H11 Agar complemented with ADC (Difco, Becton Dickinson). CFU were counted after 3 weeks of incubation at 37°C. After fixation in 10% neutral buffered formalin for 24h–48 h, lung left lobes were embedded in paraffin for 4- $\mu$ m sectioning according to standard procedures and stained in hematoxylin and eosin (HE). Stained slides were evaluated with Axioscan Z1 and Zen software (Zeiss). In another protection experiment female C57BL/6 mice were primed (s.c.) with  $1 \times 10^9$  TU/mouse of LV::li-HAEP and then boosted i.n. with the same dose of LV::li-HAEP adjuvanted with 10  $\mu$ g/mL of cGAMP. The challenge was performed i.n. with 20  $\mu$ L/mouse of a suspension of  $5 \times 10^4$  CFU/mL of Mtb H37Rv to deliver  $1 \times 10^3$  CFU/mouse.

### Mycobacteria

Mtb (H37Rv strain) or BCG::ESX-1<sup>Mmar</sup> (Groschel et al., 2017), were cultured to exponential phase in Dubos broth, complemented with Albumine, Dextrose and Catalase (ADC, Difco, Becton Dickinson, Le Pont-de-Claix, France). Non-Beijing and Beijing clinical Mtb isolates, representative of the most prevalent genotypes in France, have been submitted to the National Reference Centre for TB for drug-resistance characterization and Mycobacterial Interspersed Repetitive-Unit-Variable-Number Tandem-Repeat (MIRU-VNTR) genotyping (Allix-Beguec et al., 2008). Mtb clinical isolates were grown in Dubos broth, complemented with oleic ADC (OADC, Difco). Titers of the mycobacterial cultures were determined by OD<sub>600</sub> measuring. Experiments with pathogenic mycobacteria were performed in BSL3, following the hygiene and security recommendations of Institut Pasteur.

## METHOD DETAILS

### Transfer LV plasmids encoding Mtb antigens

Codon-optimized genes encoding EsxH alone or in fusion with the li, TFR, and MITD or encoding li-HAEP or li-HAEP were synthesized by Eurofins were then cloned downstream of the “SP1” promoter: (i) based on human  $\beta$ 2 microglobulin ( $\beta$ 2 m) promoter which

derives antigen expression predominantly in immune cells and notably activated APCs (70), and (ii) containing inserted/substituted regions originated from the CMV promoter albeit with minimal proximal enhancers and thus improved vector safety (our unpublished results). The promoter is located between BamHI and XhoI sites of the pFLAPΔU3 transfer plasmid (Zennou et al., 2000) (Figure S1), containing a mutated WPRE (Woodchuck Posttranscriptional Regulatory Element) sequence to increase gene transcription. Production and titration of LV were performed as described elsewhere (Ku et al., 2021d).

### MHC-I or -II restricted antigen presentation

Histocompatible bone-marrow derived DC were plated at  $5 \times 10^5$  cells/well in 24-well plates in RPMI 1640 containing 5% FBS. When adherent, cells were transduced with LV vectors, or were loaded with 1 μg/mL of homologous or control synthetic peptides. At 24 h post infection  $5 \times 10^5$  appropriate T-cell hybridomas were added and the co-culture supernatants were assessed for IL-2 production at 24 h by ELISA. In this assay, the amounts of released IL-2 is proportional to the efficacy of antigenic presentation by MHC molecules. The peptides harboring MHC-I or -II-restricted epitopes were synthesized by Proteogenix (Schiltigheim, France) and were reconstituted in H<sub>2</sub>O containing 5% Di-Methyl Sulfoxyd (DMSO) (Sigma-Aldrich). When indicated antigenic presentation was assessed by use of reporter T-cell hybridomas, transduced to emit fluorescent signals subsequent to TCR triggering, as recently described (Sayes et al., 2018).

### Intracellular cytokine staining

Splenocytes from immunized mice were obtained by tissue homogenization and passage through 100-μm nylon filters (Cell Strainer, BD Biosciences) and were plated at  $4 \times 10^6$  cells/well in 24-well plates. Lungs were treated with 400 U/mL type IV collagenase and DNase I (Roche) for 30 min at 37°C and homogenized by use of GentleMacs (Miltenyi). Cells were then filtered through 70-μm nylon filters (Cell Strainer, BD Biosciences), and centrifuged for 20 min at 3000 rpm at RT without brake on Ficoll gradient medium (Lympholyte M, Cedarlane Laboratories). Lung T-cell-enriched fractions were co-cultured at  $4 \times 10^6$  cells/well with histocompatible bone-marrow-derived DC ( $8 \times 10^5$  cells/well) in 24-well plates. Splenocytes or lung T cells were co-cultured during 6 h in the presence of 10 μg/mL of homologous or control peptide, 1 μg/mL of anti-CD28 (clone 37.51) and 1 μg/mL of anti-CD49d (clone 9C10-MFR4.B) mAbs (BD Biosciences). During the last 3 h of incubation, cells were treated with a mixture of Golgi Plug and Golgi Stop, both from BD Biosciences. When indicated, PE-Cy7-anti-CD107a (clone 1D4B, BioLegend) mAb was also added to the cultures at this step. Cells were then collected, washed with PBS containing 3% FBS and 0.1% NaN<sub>3</sub> (FACS buffer) and incubated for 25 min at 4°C with a mixture of Near IR Live/Dead (Invitrogen), FcγII/III receptor blocking anti-CD16/CD32 (clone 2.4G2), PerCP-Cy5.5-anti-CD3ε (clone 145-2C11), PE-Cy7-anti-CD4 (clone RM4-5) and BV711-anti-CD8 (clone 53-6.7) mAbs (BD Biosciences or eBioscience). Cells were washed twice in FACS buffer, then permeabilized by use of Cytofix/Cytoperm kit (BD Bioscience). Cells were then washed twice with PermWash 1X buffer from the Cytofix/Cytoperm kit and incubated with a mixture of BV421-anti-IL-2 (clone JES6-5H4), FITC-anti-TNF (MP6-XT22), APC-anti-IFN-γ (clone XMG1.2) and BV605-anti-IL-17A (Clone TC11-18H10) mAbs (BD Biosciences) or a mixture of appropriate control Ig isotypes, during 30 min at 4°C. Cells were then washed twice in PermWash and once in FACS buffer, then fixed with Cytofix (BD Biosciences) overnight at 4°C. Cells were acquired in an Attune NxT cytometer system (Invitrogen) and data analysis was performed using FlowJo software (Treestar, OR, USA).

### Lung cell phenotyping

Lymphocyte-enriched lung cells from mice, injected i.v. with PE-anti-CD45 (clone 30-F11, BioLegend) 3 min before sacrifice, were prepared as described above and stained with a mixture of: (i) BV650-anti-CD3ε (clone 145-2C11, BD Biosciences), eF450-anti-CD4 (clone RM4-5, eBioscience), APC-anti-CD8 (clone 53-6.7, eBioscience), PE-Cy7-anti-CD27 (clone LG.7F9, eBioscience) and AF700-anti-CD62L (clone MEL-14, BD Biosciences) mAbs, or (ii) PerCP-Cy5.5-anti-CD3ε (clone 145-2C11, eBioscience), PE-Cy7-anti-CD4 (clone RM4-5, BD Biosciences), APC-anti-CD8 (clone 53-6.7, eBioscience), BV605-anti-CD69 (clone H1.2F3, BioLegend), BV711-anti-CD103 (clone 2E7, BioLegend), AF700-anti-CD44 (clone IM7, BioLegend) and FITC-anti-CXCR3 (clone CXCR3-173, eBioscience) mAbs, all in the presence of FcγII/III receptor blocking anti-CD16/CD32 (BD Biosciences) and Near IR Live/Dead (Invitrogen). After 25 min incubation at 4°C, the cells were washed twice in FACS buffer and fixed by incubation with Cytofix (BD Bioscience) overnight at 4°C.

### Analysis of lung innate immune cells

Lungs from mice injected i.v. with PE-anti-CD45 mAb (clone 30-F11, BioLegend) 3 min before sacrifice, were treated with 400 U/mL type IV collagenase and DNase I (Roche) for 30 min at 37°C and homogenized by use of GentleMacs (Miltenyi). Cell suspensions were then filtered through 70 μm-pore filters (Cell Strainer, BD Biosciences), treated with Red Blood Cell lysis buffer (Sigma), then washed and centrifuged at 1300 rpm for 5 min. Near IR Live/Dead (Invitrogen), FcγII/III receptor blocking anti-CD16/CD32 (clone 2.4G2, BD Biosciences), APC-anti-CD11b (clone M1/70, BD Biosciences), PE-Cy7-anti-CD11c (clone N418, eBioscience), BV711-anti-CD103 (clone 2E7, BioLegend), BV421-anti-CD64 (clone X54-5/7.1, BioLegend), FITC-anti-CD24 (clone M1/69, BD Biosciences), PerCP-Cy5.5-anti-MHC-II (clone M5/114, BD Biosciences), FITC-anti-Ly6G (clone 1A8, BioLegend) and BV605-anti-Ly6C (clone HK1.4, BioLegend) were used to detect DC, macrophages, monocytes and neutrophils. Cells were incubated for 25 min at 4°C, washed with PBS + 3% FBS and fixed with Cytofix (BD Biosciences) overnight at 4°C.

### Identification of LV-transduced lung cells

Lungs from mice immunized i.n. LV::GFP with were prepared as described above and the recovered cells were stained as follows: (i) To detect conventional DC and macrophages, Near IR Live/Dead (Invitrogen), Fc $\gamma$ II/III receptor blocking anti-CD16/CD32 (clone 2.4G2, BD Biosciences), BV605-anti-CD45 (clone 30-F11, BD Biosciences), PE-anti-CD11b (clone M1/70, eBioscience), and APC-anti-CD11c (clone N418, Miltenyi), PerCP-Cy5.5-anti-MHC-II (clone M5/114, BD Biosciences), PE-Cy7-anti-CD24 (clone M1/69, Biolegend) and BV421-anti-CD64 (clone X54-5/7.1, Biolegend) were used. (ii) To detect T cells, B cells and plasmacytoid DC, Near IR Live/Dead (Invitrogen), Fc $\gamma$ II/III receptor blocking anti-CD16/CD32 (clone 2.4G2, BD Biosciences), BV605-anti-CD45 (clone 30-F11, BD Biosciences), PerCP-Cy5.5-anti-CD3 $\epsilon$  (clone 145-2C11, eBioscience), eF450-anti-CD19 (clone 1D3, eBioscience), PE-anti-B220 (clone REA755, Miltenyi) and APC-anti-CD11c (clone N418, Miltenyi) were used. Samples were incubated with appropriate mixtures for 25 min at 4°C, washed with PBS + 3% FBS and fixed with Cytfix (BD Biosciences) overnight at 4°C.

### ELISPOT assay

Splenocytes from individual mice were homogenized and filtered through 100  $\mu$ m-pore filters and centrifuged at 1500 rpm during 5 min. Cells were then treated with Red Blood Cell Lysing Buffer (Sigma), washed twice in PBS and counted in a MACSQuant-10 cytometer (Miltenyi Biotec). Splenocytes were then plated at  $1 \times 10^5$  cells/well in 200  $\mu$ L of RPMI-GlutaMAX, containing 10% heat-inactivated FBS, 100 U/mL penicillin and 100  $\mu$ g/mL streptomycin,  $1 \times 10^{-4}$  M non-essential amino-acids, 1% vol/vol HEPES,  $1 \times 10^{-3}$  M sodium pyruvate and  $5 \times 10^{-5}$  M of  $\beta$ -mercaptoethanol in ELISPOT plates (Mouse IFN- $\gamma$  or TNF ELISPOT<sup>PLUS</sup>, Mabtech). Cells were left unstimulated or were stimulated with 2  $\mu$ g/mL of appropriate synthetic peptides (Proteogenix) or 2.5  $\mu$ g/mL of Concanavalin A (Sigma), as a functionality control. For each mouse, the assay was performed in triplicates, according to the manufacturer's recommendations. Plates were analyzed in an ELR04 ELISPOT reader (AID, Strassberg, Germany).

### Multiplex cytokine quantification assay

Bone marrow-derived DC from C57BL/6 mice were incubated with medium (negative control), with Mtb at MOI = 3 (positive control), or LV at the high MOI of 50. Culture supernatants were collected at 24 h and filtered through 0,22  $\mu$ m. A quantification of IFN- $\alpha$ , IFN- $\beta$ , IL-1 $\alpha$ , IL-1 $\beta$ , IL-6, IL-10, CCL5 and TNF cytokines was performed by Tebu-Bio using the Q-Plex<sup>TM</sup> multiplex ELISA arrays (PBL Assay, Quantys Biosciences).

### QUANTIFICATION AND STATISTICAL ANALYSIS

Significance of differences between experimental groups was evaluated by using unpaired two-tailed parametric t test, as mentioned in each figure legend. Statistical analyses were performed using GraphPad Prism v9.0.0 (GraphPad Software, CA, USA). All results are representative of at least two independent experiments.